Reconstruction of the geology and structure of Lake Rotomahana and its hydrothermal systems from high-resolution multibeam mapping and seismic surveys: Effects of the 1886 Tarawera eruption

C.E.J. de Ronde[1], S.L. Walker[2], C. LeBlanc[1], B.W. Davy[1], D.J. Fornari[3], F. Caratori Tontini[1], B.J. Scott[4], F. H. Seebeck[1], T.J. Stewart[1], A. Mazot[4], A. Nicol[5] and M.A. Tivey[2]

1, GNS Science, 1 Fairway Drive, Lower Hutt 5010, New Zealand

2, Pacific Marine Environmental Laboratory, NOAA, 7600 Sand Point Way NE, Seattle, WA 98115-6349, USA

3, Woods Hole Oceanographic Institution, 266 Woods Hole Road, Woods Hole, MA 02543, USA

4, GNS Science, 114 Karetoto Road, RD4, Taupo 3384, New Zealand

5, Geological Sciences, University of Canterbury, Private Bag 4800, Christchurch, New Zealand

Contribution to the *Journal of Geothermal and Volcanological Research* special issue on Lake Rotomahana. Cornel E.J. de Ronde and Alessandro Aiuppa (eds).

Abstract

Present-day Lake Rotomahana represents the focal point of one of the most destructive eruptions in New Zealand's historical record, i.e., that of Mt. Tarawera on 10 June 1886, with devastating loss of life and presumed destruction of the iconic Pink and White Terraces that were perched on the margins of the lake. Basaltic dikes are considered to have ascended near surface in the area, intruding into hydrothermally altered and water-saturated ground beneath the existing lake. The consequential phreatomagmatic eruption ejected 0.5325 km^3 of material from the lakefloor and below, plastering the nearby landscape for several kms with mud and debris. The eruption buried the natural outlet of the lake, with the bottom of the craters filled by water within months and completely concealed from view within years; today Lake Rotomahana has depths up to 118 m.

High-resolution (0.5 m) bathymetric mapping, when combined with a 2-D seismic reflection survey, enables us to 'see' details of the maar craters on the lakefloor and those buried by sediment. The large Rotomahana Crater described by workers immediately after the eruption measures ~2.5 km in diameter near its southwestern end, and excavated ground to 155 m below present-day lake level. The vent system forms an array of right-stepping (dextral) craters, with the main crater host to two sub-craters today buried beneath the lakefloor; Rotomahana West Crater and Rotomahana East Crater, which are in-filled by 36 and 37 m of sediment, respectively. Subordinate craters along the same 057° trend include Hochstetter Crater (11 m of infill), Waingongongo Crater (14 m) and Rotomakariri Crater (26 m). These craters host a total volume of sediment equal to 0.0268 km^3. Other features highlighted by the bathymetric data include; craters not filled by sediment, sediment fan deltas, volcanic ridges and dikes, terraces formed during lower lake levels and gas

pockmarks, all either related to the 1886 eruptive episode or post-eruption hydrothermal and erosional processes.

Application of results from bubble plume, CO_2 flux, magnetic and heat flux surveys of Lake Rotomahana to this study, when combined with regional earthquake relocation analysis and broadband magnetotelluric data, show the effects of a heat source and corresponding convective water/heat transport system extending from a magma body located south of Waimangu to underneath the western end of the lake. The Pink Terraces hydrothermal system has survived the 1886 eruption and appears to be the eastern-most extension of a larger system that lay beneath the Waimangu area before the eruption. A holistic approach has provided a coherent context for the eruption and its effect on the historical Pink and White Terraces hydrothermal systems, the formation of the new Patiti hydrothermal system, and the relationship of craters within Lake Rotomahana to those of Mt. Tarawera and Waimangu.

Keywords: Lake Rotomahana; Rotomahana West, Rotomahana East, Hochstetter Waingongongo and Rotomakariri Craters; Pink Terraces and Patiti hydrothermal systems.

Introduction

On 10 June 1886, Mt. Tarawera erupted, forever changing the landscape in the near vicinity of this volcano and ensuring a place in New Zealand history, taking the lives of 120 inhabitants and presumably destroying the iconic Pink and White Terraces, considered at the time to be one of the 8 natural wonders of the world. Fortunately, practical photography as a commercially available interest was introduced in 1839, ensuring that the Terraces were captured for perpetuity in all their

glorious detail prior to the eruption. In addition, the advent of photography meant that the effects of the 1886 eruption in the general Lake Rotomahana area were precisely (accurately) recorded, in concert with surveys and expeditions made by various groups immediately post-eruption (see Keam, this issue).

The eruption of Mt. Tarawera began around 2:00AM on June 10 1886, with the explosions at 3:30 AM considered to be the outbreak at Rotomahana. The violent magmatic stage of the eruption ended around 6:00AM (Keam, this issue, and references therein). In the days that followed the eruption, various groups visited the region, including one journalist who described how the original lake was gone with no remnant of the famed Terraces that could be discerned. Instead, he described a "…great crater over a mile [>1600 m] long and half a mile [800 m] wide…" with "…dense volumes of steam and smoke, with a din and a roar and rattle baffling description…". At least 11 separate orifices, or small craters, were seen to be ejecting rock fragments high into the air along the western end of the crater (T.W. Leyes, 1886, as referenced by Keam, this issue).

Today's Lake Rotomahana began forming within the largest of the craters shaped by the eruption soon after they were established. Historical records show that the lake level rose most rapidly in the first few decades after the eruption, with the last 80 years having fluctuated between 332 and 342 m above sea level (a.s.l.) (Keam and references therein, this issue). Thus, no person has laid eyes on the volcanic structures and associated geothermal manifestations attributed to the 1886 eruption for over 100 years. Today, the application of state-of-the-art techniques, such as high-resolution multibeam mapping of the lakefloor, when combined with two dimensional (2-D) seismic reflection profiles, not only affords us the opportunity to both 'see' the lakefloor as if there were no lake present, but also below the lakefloor

and the ground surface at the time of the 1886 eruption. This relatively rare use of modern investigative techniques in a lake, commonly reserved for marine surveys, means we can for the first time since 1886 reconstruct the volcanological aftermath of the 1886 eruption as it displaced the original Lake Rotomahana, and document both the evolution of pre-existing geothermal systems and the birth of any new ones following the eruption. Moreover, relatively few volcanic lakes deeper than 30 m have been studied for their hydrothermal emissions, including; Crater Lake, Oregon (Dymond et al., 1989) and Yellowstone Lake, Wyoming (Remsen et al., 1990) in the USA, Lake Baikal in Siberia (Crane et al., 1991), Lake Tanganyika in East Africa (Tiercelin et al., 1993) and Lake Taupo in New Zealand (de Ronde et al., 2002). Thus, this study, which includes sublacustrine venting of Lake Rotomahana, adds to our inventory of hydrothermal processes occurring within volcanic lakes.

Okataina Volcanic Centre

The Okataina Volcanic Centre (OVC) comprises an area of ~700 km^2 within the Taupo Volcanic Zone of New Zealand east of Lake Rotorua (Fig. 1). It is comprised largely of the Okataina Caldera which is considered to have collapsed around ~280,000 years ago, as given by Ar/Ar dating of the Matahina Ignimbrite (Houghton et al., 1995), the first widespread volcanic formation originating within the OVC (Nairn, 2002). The present-day margins of the southern half of the Okataina Caldera are considered to have formed by 220,000 years ago. The northern part of the Okataina Caldera is considered to have collapsed around 65,000 years ago with the eruption of the Rotoiti Pyroclastics eruption (Nairn, 2002). In all, it is thought that the OVC has erupted ~2000 km^3 of magma over the past 65,000 years, making it one of the most productive rhyolite volcanic centers ever documented (Wilson et al.,

2009). A series of intra-caldera lava and pyroclastic eruptions has occurred in the OVC during the past 22,000 years, including the progressive building of the rhyolite domes of the large Haroharo Volcanic Complex to the north and the large Tarawera Volcanic Complex to the southeast (see Fig. 1). For additional details concerning the OVC, see de Ronde and Scott (this issue).

Lake Rotomahana structural and tectonic setting

Lake Rotomahana is located within the Tarawera Linear Vent Zone (TLVZ) as part of the OVC (Fig. 1). The vent system occurs along the southeastern margin of the Taupo Volcanic Zone and the intra-arc Taupo Rift. Rift faults formed over the past 1.6 Myr (Wilson et al., 1995) in response to steepening and/or rollback of the subducting Pacific Plate and clockwise rotation of the eastern North Island (Wallace et al., 2009; Seebeck et al., 2014). At ground surface, the Taupo Rift comprises a dense network of active NE-SW striking and steeply dipping normal faults (>60º) with vertical displacements of up to 550 m (Villamor and Berryman, 2001; Nicol et al., 2010; see Fig. 1). Some active normal faults extend into the OVC where they become buried by volcanic deposits (Seebeck et al., 2010). Outside of the OVC, extension and crustal thinning is considered largely due to rift faulting (Nicol et al., 2006, 2010; Villamor et al., 2011), while within the volcanic center crustal extension is thought to be a combination of dike intrusion and normal faulting (Rowland et al., 2009; Seebeck and Nicol, 2009). The TLVZ is 28 km long and 5 km wide and is inferred to overlie a basic intrusion associated with the basaltic eruptives at Waimangu, Rotomahana and Tarawera (Cole 1973). The two most recent eruptions from the TLVZ (i.e., 1315 AD and 1886 AD) were accompanied by intrusion of basaltic dikes ≤5 m wide in the near surface, along the axis of the system (Smith,

1886; Nairn and Cole, 1981; Rogan and Hochstein, 1984; Nairn et al., 2005). The 17 km long 1886 Tarawera Rift lies within the TLVZ (Nairn and Cole 1981, Nairn 2002). During the 1886 AD eruption of Mt. Tarawera the dike(s) and associated phreatic eruptions extended along the vent system for 17 km, terminating within 1 km of active faults in the Taupo Rift (Fig. 1).

Lake Rotomahana geology

Volcanic units outcrop around the margins of Lake Rotomahana. The very western end of the lake has outcropping <65 ka rhyolite domes and flows and undifferentiated pyroclastic fall, flow and surge deposits of the Okataina Rhyolite and Haparangi Rhyolite Pyroclastics, respectively (Nairn, 2002). The northeastern shoreline, parts of the southeastern shoreline and Patiti Island reveal various units ascribed to volcanic events ranging in age between ~22 ka and 15 ka (Nairn, 2002), including pyroclastic surge deposits (Fig. 2A) and rhyolite lava (Fig. 2B). Other prominent outcrops include the 0.7 ka 'Green Lake Plug' (Fig. 2C) that separates Green Lake Crater from Lake Rotomahana in the very northeastern end of the lake. Rotomahana 'mud' that was expelled during the June 10 1886 eruption can be seen in northwestern and southern parts of the lakeshore, including a recently exposed example in a road cut (Fig. 2D), as part of the Rotomahana Pyroclastics Member (Nairn, 2002).

Lake Rotomahana hydrothermal activity

Geothermal manifestations seen along the margin of Lake Rotomahana largely occur on the western shoreline of the lake; minor hot springs also occur along parts of the southern shoreline southwest of Patiti Island and directly south of Awarua Cliffs,

and along a short distance near "bubble rock" on the lake margin north of Patiti Island. The hot springs are near-neutral pH, alkali chloride waters that are typically boiling, or near boiling (see Stucker at al., this issue). Displays noted along the western shoreline include the Steaming Cliffs, which mark the subaerial portion of Donne Crater, with associated hot springs near the water's edge (Fig. 3A). Fumaroles are also commonplace, especially along Awarua Cliffs in Fumarole Bay (Fig. 3B). Boiling hot springs and miniature geysers are also notable on the western margin of Donne Crater, typically occurring within a few m of the lake (Fig. 3C). Some of these geysers derive from spectacular sinter forms, such as the Angel Wings Geyser (Fig. 3D) with adjacent hot springs and silica sinter abounding in the near vicinity. The degree of activity of the more prominent geysers is largely controlled by lake level, with the Otukapuarangi Bay Geyser (Fig. 3E) the most active geyser during the survey period. However, bubble plumes rising from the lakefloor are arguably the most common expression of hydrothermal activity in the area, and are especially vigorous just offshore the western shoreline of the lake (see Fig. 15 later). For location of the various features mentioned above, see Figure 4. For details on the methods employed and techniques used in the various surveys mentioned below, including data reduction and presentation, see Appendix I.

Bathymetric survey

Lake Rotomahana covered an area of 8.89 km^2 at the time of our survey, which includes a very shallow (< 5 m), relatively large area in the very southern part of the lake, and other smaller areas in the northeastern, northwestern and southwestern parts of the lake (Fig. 4). Its longest length in a NE-SW direction is 6.70 km and longest width in a NW-SE direction 3.12 km, as calculated using an Albers Equal Area

projection; the lake outline shown in Figure 4 and elsewhere is from the Land Information New Zealand data service as part of the Topo50 1:50,000 scale map series.

The lake was first surveyed by single beam echo sounding over three days in October 1978 (Irwin, 1982). Track line spacing for that survey averaged ~200 m, or equal to a resolution of the lakefloor bathymetry of ~200 m. The deepest part of the lake in the Irwin (1982) survey is depicted as a 112.4 m bathymetric contour.

Between 24 January and 2 February 2011, two *Remus 100* AUVs (autonomous underwater vehicles) were deployed in Lake Rotomahana to map in high resolution both the lakefloor and water column using various sensors (see de Ronde et al., this issue; Walker et al., this issue). The AUVs completed 18 missions between them and covered 300 line km's within the lake during 73 hours in the water. The main objective of the vehicle *Darter* was to acquire 3D bathymetric data using an *Imagenex* Delta-T 675 kHz downward looking multibeam sonar. However, due to intermittent performance issues, later determined to be damaged internal electronics on the receiver side, the mission was changed with tighter row spacing while combining altimeter and depth data from each vehicle and using these data as a 'single-beam' bathymetric data set. The data from both vehicles were combined and gridded at 15 m to provide a bathymetric data product about 13 times higher resolution than that of Irwin (1982), covering an area of 4.26 km^2, or ~48% of the total lake area. However, while the AUV data showed tantalizing features on the lakefloor unresolvable from the Irwin (1982) map, including an area around the Pink Terraces (see https://www.youtube.com/watch?v=po53v4TGPbc), the resolution was still considered too coarse to be able to map geological features with any detail. Hence, it was decided undertake a more detailed survey at higher resolution and better coverage.

Results

A total of 141 km of survey lines were completed in 2012 by iXSurvey, with almost 95 million soundings measured (see Appendix I for details). The maximum depth recorded in the lake was 118.06 m. The area of the lake covered during this survey was 7.57 km^2, or equal to 85% of the lake area, with only the above-mentioned very shallow areas not surveyed. The bathymetric grid used to create Figure 4A was produced at a resolution of 0.5 m, or 400 times better resolution than that of Irwin (1982) and 30 times better than the AUV survey, and reveals startling details of the lakefloor, especially around the lake margins. The very center of the lake has clearly been in-filled by sediments over the 126 years that have elapsed between this survey and the eruption in 1886, and has a relatively flat bottom covering 1.72 km^2 when enclosed by the 105 m contour. This basin, here termed the Rotomahana Basin, is punctuated on its southern margin by a zone measuring ~500 m by ~230 m (or an area of ~0.094 km^2) containing numerous pockmarks trending about 057° (Fig. 4B) that can be attributed to gas escape structures (Fig. 5A; see below). South of here is a large sublacustrine fan delta comprised of re-worked eruption products such as mud and ash that have been washed into the lake from the surrounding hillsides (Fig. 5B). Similarly, another delta occurs just west of here and again on the opposite (northern) side of the lake in concert with streams that drain the nearby hills. These deltas are affected by slumps and together with other areas in the lake—but especially the shallower areas NE of the Rotomahana Basin—are bisected by numerous channels likely representative of streams and rivulets that dissected the ash-covered slopes prior to the lake rising to its present level. A smaller, flat-bottomed basin in the very NE part of the lake, termed Rotomakariri Basin by Irwin (1982), covers an area of

0.16 km^2 when enclosed by the 70 m contour.

The bathymetry of Lake Rotomahana is also notable for a number of sharply defined ridges that locally strike into the lake from its margins, in part from promontories around the lakeshore. This is particularly well seen in the area of the Pink Terraces and its surrounds in the northwestern part of the lake (Fig. 5C), the area of the White Terraces on the northern side of the lake, and in an area ~1.5 km east of the latter, also on the northern side of the lake (see Figs. 1B and Fig. 4B).

Arguably the most striking features of the high-resolution bathymetry of Lake Rotomahana are the numerous craters seen on the lakefloor. The most obvious occur on the far western side of the lake and in an area north and northeast of Patiti Island (Fig. 4B). These include four large, circular craters around the margin of the lake that range in diameter from 332 to 452 m if we include their subaerial component, with 'depths' from their rims to crater floors between 67 and 84 m (Table 1). By contrast, clusters of smaller craters (e.g., Fig. 5D) have diameters ranging between 37 and 85 m and rim-to-crater-floor depths of 6.8 to 20.4 m. An intermediate size group of three craters NE of Patiti Island have diameters between 146 and 162 m and rim-to-crater-floor depths ranging between 27.8 and 52.1 m (e.g., Fig. 5E). Many of the craters are complete in form, whilst others appear to have only remnants of their postulated crater walls (cf. Figs. 4A and B). Other craters may be buried beneath the sediment, although seismic surveys show that only a relatively thin veneer of sediment occurs outside the basins of the central and far northeastern parts of the lake (see below). However, a possible large crater (~355 m in diameter; 1.5 m depth) is barely discernable immediately SW of Patiti Island, with a seismic section through the area (not shown) suggesting that this may indeed be a shallow crater largely in-filled by sediments (Fig. 4B). Of the 15 craters measured and presented in Table 1, ten have

ratios of their diameter to depth between 4.0 and 5.4, implying similar mechanics and conditions in their formation. Three other craters with higher ratios between 6.7 and 8.5 are likely skewed because of greater sediment infill, with the aforementioned large crater with a ratio of 237 almost completely buried.

Our high-resolution bathymetric map affords us the opportunity to compare our results with facsimiles of paintings and old maps drawn immediately after the eruption. For example, one of the promontories seen in the bathymetric map forms the remnants of Pinnacle Ridge, as mapped by Hochstetter (1864; Fig. 4B). Immediately following the eruption in October 1886, the artist Charles Blomfield painted the 'Pinnacle', a lava neck (or dike) thought to be located somewhere in the vicinity of the northern part of the old Pinnacle Ridge. What is remarkable is that by comparing the high-resolution bathymetric map in this area with the painting by Bloomfield we can see the two are clearly the same structure (Fig. 6), thus locating an important landmark of post-eruption Lake Rotomahana.

Similarly, photographs taken of the Lake Rotomahana area immediately post-eruption have proved invaluable in establishing the lie of the land and indeed, details of various volcanic edifices. For example, Star Hill Crater was photographed by Burton Brothers in late July / early August 1886 (Keam, this issue). Comparison with the bathymetry shows that approximately the bottom half of this crater has been flooded by the lake. If we add the surrounding digital terrain topography, the match is startling, even to the point of the fumaroles situated on the outside flank of the crater (right foreground of the photograph) correlating with pockmarks on the bathymetric map (Fig. 7).

The map drawn by S. Percy Smith of the Rotomahana Crater clearly shows a crater south east of Star Hill Crater that is likely the crater shown in Figure 5E. Moreover,

in July 1886, Smith (1887) writes "…Partially connected to Green Lake crater there was next a continuous two-kilometer-long rift that, when discovered in late July 1886, was already occupied by water, and formed the largest lakelet ('Rotomakariri') that had collected within the craters to that time. Further to the southwest the crater edges, bounding this feature and also bounding a fairly densely packed distribution of vents beyond it, gradually diverge…". The latter vents are likely those shown in Figure 5D; reference to the lakelet 'Rotomakariri' and it shape, depicted as two lobes on the map made by Smith, almost certainly relate to the Rotomakariri and Waingongongo Craters that are today buried by sediment (see below).

Finally, a series of terraces can be traced around the lake margin and also occur on the edge of Patiti Island, to depths of ~19 m (Table 2). Many of the terraces occur in several places throughout the lake, with prominent examples occurring immediately north of the Pinnacle (Fig. 5F) and SE of Patiti Island (Fig. 4B). Up to 14 terraces can be discerned from the bathymetric data, with the subtlest best differentiated in cross section (Fig. 8).

Lakefloor photography

A number of camera stations were occupied during the 2011 (n = 16) and 2014 (n = 18) field campaigns on Lake Rotomahana, especially over the inferred Pink and White Terraces areas, but also areas where the bathymetry showed prominent volcanic edifices and/or where bubble plumes were known to rise from the lakefloor (Fig. 3F; see below). A total of 5130 photographs were taken by the cameras between the two surveys, with a small percentage capturing useable images of the lakefloor, effectively ground-truthing the exposed geology. For location of the camera stations occupied during this study see Fig. 9A; details of the camera system are in Appendix I.

Results

The lakefloor at Rototmahana is invariably covered by sediment, especially away from the steep slopes surrounding the lake margin. Typically, an orange-yellow colored flocculent sits on top of darker, carbonaceous material (Fig. 10A), where locally evidence for ripples can be seen, implying currents within the lake (Fig. 10B). The orange-yellow flocculent material is host to plant matter and the occasional worm and is marked by bioturbation (Fig. 10C). It is clearly underlain by black organic-rich material, which itself is underlain by a grey colored, finer grained sediment (Fig. 10E) that is considered to be Rotomahana Mud, or part of the Tarawera Tephra deposited from the 1886 eruption (Muir, 2012).

Outcrops of rock invariably occur around the lake margin, and especially in the western and northern parts of the lake where noticeably steep ridges are apparent in the bathymetry (Fig. 4B). Commonly seen in various parts of the lake is a mostly massive, rough-textured unit with local crude layering (Fig. 11A), which can host various size clasts (Fig. 11B), and likely represents the Rotomahana Mud ejected out of the old lake bed during the 1886 eruption. Also common are layered units of pyroclastic material (Fig. 11C) that can locally show evidence for hydrothermal alteration and which can also host relatively large (up to 0.5 m) blocks of unaltered volcanic rock embedded in the matrix (Fig. 11D). In the area of the Pink Terraces (Fig. 1B), the unaltered Rotomahana Mud clearly sits ontop of hydrothermally altered volcanics (Fig. 11E); in this same area other examples of the latter appear to host blocks of lava that are unaffected by hydrothermal alteration (Fig. 11F). In some instances, the blocks contained within this unit can be up to 1 m wide (Fig. 11G). A rare example of lava is seen in the Pinnacle area (see Figs. 11H and Fig. 4B).

The discharge of gas and hot water into Lake Rotomahana is extensive, although is mostly concentrated in an area just offshore the western margin of the lake, where the Pink Terraces geothermal activity was widespread prior to the 1886 eruption (Fig. 1B). It is also prevalent in the southern part of the lake, and to a lesser degree in the Pinnacle area where the White Terraces once stood (Figs. 1B and 4B), and in two areas north and northeast of Patiti Island (see Fig. 15 later).

Plumes of bubbles rising from the lakefloor are the most common sublacustrine manifestation of geothermal activity in the lake (e.g., Fig. 3F) and when seen on the lakefloor, can originate from more isolated vents (Fig. 12A) that locally discharge hot water (Fig. 12B), through to high density vent areas around the highest heat flow zone measured in the lake (Fig. 12C), to quite large (up to 1 m diameter) vents (or pockmarks) in the southern part of the lake (Fig. 12D). Elsewhere, crusts can be seen to mantle highly altered volcanic rocks (Fig. 12E) that locally show extensive thicknesses of hydrothermal alteration (Fig. 12F). Closer inspection shows some of the surfaces of the altered rocks to host intricate textures (Figs. 12G and H), possibly related to liesegang weathering prior to the lake rising.

Seismic surveys

A number of two dimensional seismic lines were surveyed over Lake Rotomahana using a Boomer system (see Appendix I), ensuring an extensive coverage over the lake. Tracks oriented parallel to the lake axis were spaced between 100 and 200 m, including Line 100 that runs down the very center of the lake, while those running across the lake were spaced between 80 and 400 m (Fig. 9B). A much more dense set of lines was surveyed over the Pink Terraces area, which will be discussed in de Ronde et al. (this issue). In total, ~150 km of Boomer seismic line data were

collected during this study. The overall quality of the Boomer lines is good despite the steep slopes and high concentrations of gas in the water column/sediments.

Results

An opportunity to compare the velocity of sound through the water column was done by combining seismic reflection and bathymetric data. That is, using bathymetric depths for the lake between 22 and 117 m, a strong correlation (R^2 = 0.999) occurred between different data sets using a velocity of 1470 m/s for the water column, essentially the same as the 1468m/s value measured during the bathymetric survey for depths ≥30 m. We then use 1600 m/s for the velocity of volcaniclastic and sedimentary material that fills the center of the lake as a result of post-eruption collapse of the crater margins into the basin, and subsequent infilling with material supplied by runoff and streams surrounding the lake. This is consistent with the velocity used for similar material infilling nearby Lake Tarawera (Davy and Bibby 2005).

Track Line 100 is oriented down the center length of Lake Rotomahana (Fig. 9B) and is the longest survey line over the lake. The two dimensional section of Line 100 is shown in Figure 13A, with the interpreted boundary between the 1886 Tarawera eruption sediments and the underlying volcanic/sedimentary terrain determined by a widespread, conspicuous reflector that could be mapped consistently in 3 dimensions, and which in general formed the lowest mappable horizon. Determining the position of this reflector was aided by reviewing seismic sections both adjacent to Line 100 and those that crossed this line in the near vicinity (see Fig. 9B). This was, however, locally complicated with masking by high amplitude, flat-lying gas layers within the stratigraphy. Phreatomagmatic surge and rhyolite lava deposits, together with local

slumping, may also complicate the interpretation of the base Tarawera 1886 surface and thus the interpreted horizon may under estimate the horizon depth and unit volume in places. However, given that the volumes calculated independently from seismic and outcrop mapping are comparable (see below), we believe any uncertainty in the mapped horizon would not significantly impact the first-order conclusions of the interpretation.

A distinct, steep margin can be seen in the western end of the section, followed by the Rotomahana Basin where sediments notably infill two craters—hereafter referred to as West Rotomahana Crater and East Rotomahana Crater—with an intervening topographic 'saddle' in between. Thereafter, the section crosses Smith Crater and others NE of Patiti Island (e.g., Fig. 5E) then a shallow basin—hereafter referred to as the Waingongongongo Basin[†]—and finally Rotomakariri Basin in the far northeastern end of the lake (both underlain by craters of the same name). A smaller, inferred crater also filled with sediment occurs just southwest of Waingongongongo Basin, hereafter referred to as Hochstetter Basin (Fig. 13B) but which in not easily discernable in the bathymetry (Fig. 4B).

Applying a velocity of 1600 m/s for sediment infilling Rotomahana Basin, we calculate a maximum thickness of 37 m for East Rotomahana Crater; using regionally unrealistic velocities of 1500 m/s or 2000 m/s as end-member P-wave speeds through volcaniclastic rocks results in a range of maximum sediment thicknesses from 34 to 46 m, respectively. Similarly, Rotomakariri Crater, Waingongongongo Crater, Hochstetter Crater and West Rotomahana Crater have maximum sediment thicknesses of 26, 14, 11 and 36 m, respectively. Seismic sections showing sediment thickness

[†] The gently sloping alluvial plain extending from Pinnacle Ridge and pre-eruption Lake Rotomakariri to the foot of Tarawera mountain (see Keam this issue), according to Hochstetter's 1859 map, was named "Te wai ngo ngo ngo ngo" by S. Percy Smith in his 1886 report on the eruption (p. 42), who renders this as "Waingongongongo".

across the lake are shown in Figure 14 where thicknesses of the sediment in Rotomahana Basin are consistent with those shown in Figure 13. Thus, our estimate for the maximum depth to 'basement' for the Rotomahana craters is around 155 m beneath the current lake level, i.e., a maximum water depth of 118 m + a maximum sediment thickness of 37 m = 155 m.

Members of a party viewed the aftermath of the eruption through old Lake Rotomahana three days after the event, with one Thomson W. Leys commenting "…but the lake was gone – not only the water, but the bottom driven out, scooping the bed to a depth of at least 250 feet [76 m] below the old level…The great crater was over a mile [1600 m] long and half a mile [804 m] wide." (from Keam, this issue). Using the postulated 1886 eruption surface in Line 100 (Fig. 13), the main crater prior to sediment infill is between 1800 and 2200 m long, depending on what reference points are used to mark the margins of the crater. Similarly, Line 500b would have been closest to the viewing party and measures about 750 m across between the foot of the southeast slope and part way up the northwest slope bounding the basin, similar to the observation made by Leys. However, both sections depicted in Lines 500b and 303 show striking, well defined steep margins that are related to the excavation of the craters from the phreatomagmatic eruption through Lake Rotomahana; this is seen at the SE end of Line 500b and at the NW end of Line 303 (Fig. 14). Using the shallower parts of these margins as bounds for the width of the crater through the lake, we get ~1150 m for Line 303 immediately west of Patiti Island and ~1400 m from Line 500b in the SW of the lake (Figs. 9B and 14), consistent with a gradual diverging of the "…outer crater margin…" from NE to SW, as observed by Smith (1887, as quoted in Keam, this issue). These are minimum values as the rift margins are still rising at the end of the seismic sections, as they approach the lakeshore.

The pre-1886 lake level has been quoted as 292 m above sea level (a.s.l.; Keam, this issue), which means the crater was excavated down to 216 m a.s.l. following the observation of Leys. However, with the lake level at 340 m during our survey, a maximum water depth of 118 m and a maximum sediment thickness of 37 m in the Rotomahana Basin, this is equal to 185 m a.s.l. at the bottom of the main crater. Thus, if the quoted 76 m for excavation of the main crater is accurate it will have occurred from *below* the bottom of the old Lake Rotomahana, which in turns implies that the lake was up to 31 m deep before the eruption. For the sediment accumulated in Rotomahana Basin shown in Figures 13 and 14 to be 76m thick we would need to use a velocity of 3400 m/s, which is unrealistic.

Bubble plume survey

A survey to map the distribution of bubble plumes throughout the lake was undertaken as a means of tying present-day hydrothermal activity to the geology and structure of the lake, as determined by the above-mentioned bathymetric and seismic surveys, respectively. This complements the CO_2 flux survey of Mazot et al. (2014) and ^{3}He measurements of Stucker et al. (this issue).

Results

A total of ~750 separate bubble plumes (predominantly CO_2 in composition; Mazot et al., 2014) were recorded during the survey (Fig. 15), dominated by strong and moderate plumes, with lesser weak, diffuse and very strong plumes. This is a minimum, as other plumes may exist between the 30 m spaced lines of the survey (Fig. 9C), although the general pattern of plume distribution is unlikely to change with a higher density survey. Water depth will play a role in the type of plume

recorded by the sounder, given the criteria used to determine each type of plume (see Appendix I). Even so, the different types of plumes were seen in a range of depths throughout the lake. Thus, the survey provides a good first-order measure of both the distribution and flux of gases into the lake.

There are two dominant areas of bubble plumes in Lake Rotomahana; one that extends up to 800 m off the western shoreline of the lake and which stretches ~1300 m along that shoreline from just north of Otukapuarangi Bay to south of Donne Crater (Fig. 4B)—hereafter referred to as the Pink Terraces hydrothermal system—and a second that spans a zone up to 700 m wide and 1500 m long—hereafter referred to as the Patiti hydrothermal system—that strikes WSW between the southwest corner of Patiti Island and the southwestern part of the lake (Fig. 15). The plumes in both of these areas are dominated by moderate and strong plumes, with a few very strong plumes dispersed within the Pink Terraces area and a small number of weak and diffuse plumes found in both areas.

Intermediate between the above-mentioned two areas of densely distributed bubble plumes is a smaller area of plumes located around the mooring site (see Walker et al., this issue), centered ~700 m north of the southern lake shoreline, SE of Donne Crater (see Figs. 4B and 15). Gas discharge here is dominated by strong and very strong plumes.

Other, minor areas of plumes were recorded, in a clockwise direction; 1) in the Pinnacle area (where the White Terraces are believed to have once stood), 2) a couple of areas further eastwards around 'bubble rock', 3) an area over a cluster of small craters NE of, but closer to, Patiti Island, 4) another area over moderate-sized craters NE of Patiti Island, and 5) a small area immediately offshore the southern shoreline of the lake (see Figs. 4B and 15). With the exception of only weak plumes above the

aforementioned small craters NE of Patiti Island and proportionally more strong plumes at the mooring site, there is no obvious preferred distribution of plume types throughout the lake.

Discussion

The accumulation of a wealth of new information relating to the geology, structure, geophysical anomalies and water column measurements at Lake Rotomahana allows us more than ever before to assemble the pieces of post-1886 hydrothermal activity in the lake.

Interpretation of bathymetry

The high-resolution bathymetric map of Lake Rotomahana (Fig. 4A) reveals numerous volcanic craters and other manifestations that can be attributed to the effects of the 1886 Tarawera eruption through this area. The craters visible on the lakefloor, in concert with the known craters in-filled by sediment (e.g., Fig. 13), have all the hallmarks of a maar volcanic complex with broad, low-relief volcanic craters formed by phreatomagmatic eruption, i.e., an explosion caused by hot lava, or magma coming into contact with ground water or a hydrothermal system. In this case, basaltic dikes are considering to have intruded beneath old Lake Rotomahana and Lake Rotomakariri (Fig. 1), triggering the catastrophic eruption (Nairn and Cole, 1981; Keam, 1988). Country rock fragmentation and crater excavation below ground surface are characteristic features of maar volcanoes and their surrounding ejecta rings comprise up to 90% non-juvenile lithic fragments (e.g., see Pittari et al. and May et al., this issue, and references therein). A maar characteristically fills with water to form a relatively shallow crater lake. However, in this case the depth of the

lake is significantly greater due to the eruption sealing off Kaiwaka stream, the historical drainage route for pre-1886 Lake Rotomahana into Lake Tarawera (Keam, this issue). Hydrothermal explosions are reported to have continued for several weeks after the eruption, with large volumes of steam expelled from the vents for several months until they became drowned by the newly forming lake (Keam, this issue and references therein).

The main Rotomahana Basin in the centre of the lake, and the smaller Rotomakariri and Waingongongongo Basins in the northeastern end of the lake, completely infill the largest craters borne from the 1886 eruption (Keam, this issue; see below). The largest *visible* craters, with the exception of the one inferred to be almost completely buried by sediment SW of Patiti Island (Fig. 4B), are today all found on the margins of the lake in two main areas; north of Patiti Island (e.g., Fig. 7) and along the western shoreline of the lake (Fig. 4B). Smaller sized craters occur in clusters and are more common (e.g., see Figs. 5D and E). If we include the largest craters buried by sediment, there is a suggestion of increasing frequency of explosion craters as crater diameter decreases (Table 1), presumably indicative of the much greater energy required to form the larger craters.

In some instances, the bathymetric data can be used to fairly accurately determine local effects of the eruption. For example, the White Terraces were located on the western side of Pinnacle Ridge prior to the eruption of 1886 (Hochstetter, 1864). The crest of the northern part of this ridge is reported by Keam (this issue) to have reached an altitude of 347 m a.s.l., or rising 55 m above the old Lake Rotomahana lake level, while the crest of the southern part of the ridge had an altitude of 353 m a.s.l., rising to 61 m above the old lake. It has been suggested by Keam (this issue and references therein) and others that the 'Pinnacle' depicted in the painting by Bloomfield (Fig. 6),

and shown in numerous photographs after the eruption, is most likely a remnant of the northern part of Pinnacle Ridge. Thus, as the depth to the top of the Pinnacle today is at 16.8 m water depth, or 323 m a.s.l., at least 24 m of the old Pinnacle Ridge was removed during the eruption.

The 'wave cut' terraces that circumnavigate much of the lake (see Figs. 4B, 5F and 8) are testament to rising lake levels at Rotomahana post-1886 eruption and damming of Kaiwaka stream. However, it is possible some of the terraces might be related to higher lake levels at Rotomahana that occurred before 1886. For example, a pre-1886 lake level of 290 m has been given for nearby Lake Tarawera (Hodgson and Nairn, 2005). Consequently, Lake Rotomahana at the time would have had an additional elevation of no more than 2 m (i.e., 292 m a.s.l.) considering Maori canoe were commonly navigated down Kaiwaka stream, which connected the two lakes, then poled and pushed them back upstream (Keam, this issue). Thus, any rise above 292 m in Lake Tarawera would have resulted in a single water body that encompassed both lakes.

The so-called Greater Lake Tarawera was created when ~5500 yrs B.P. Whakatane eruptions dammed the normal lake outlet, with lake levels rising to 60 m above their normal state, stabilizing at 330 m a.s.l., then dropping down to 315 m a.s.l. over the next ~4900 years (Hodgson and Nairn, 2005). At around AD 1320, the dam blocking the normal Lake Tarawera failed and lake levels dropped again to around 290 m (and Lake Rotomahana to ~292 m). This implies that old Lake Rotomahana levels will also have risen to the same elevations as Lake Tarawera before AD 1320. Inspection of Table 2 and Figure 8 shows two prominent terraces occur near 330 m a.s.l. (Terrace 'h' located between 330.4 and 330.9 m a.s.l. and Terrace 'g' at 329.9 m a.s.l.), which in all likelihood are variations of the same terrace. Seven additional

terraces can then be seen in the lake bathymetry down to a depth of 18.7 m, or 321.2 m a.s.l., with no further terraces discernible below that depth. It is unclear, however, if these terraces can be correlated with the maximum heights of Greater Lake Tarawera, as the original landscape would have had to been preserved post-1886 eruption.

Compilation of other surveys

Combining the information derived from the high-resolution magnetic (Caratori Tontini et al., this issue), heat flow (Tivey et al., this issue), CO_2 flux (Mazot et al., 2014) and AUV water column surveys (Walker et al., this issue; see Fig. 16) with the high-resolution bathymetric map and seismic results enables a more holistic interpretation of volcanic events and hydrothermal activity related to the 1886 Tarawera eruption.

The magnetic survey of Tontini et al. (this issue) clearly shows positive magnetic anomalies on the SE side of Lake Rotomahana that can be attributed to the outcropping Matahina Ignimbrite and Haparangi Pyroclastics, and various Okataina Rhyolites, including the Patiti Island Dome (Nairn, 2002; Pattari et al., this issue). The negative anomaly in the very northeastern part of the lake is due to topographic affects (lava domes) from the adjacent countryside (not shown). By contrast, the obvious and large negative anomaly centered in the southwestern part of the lake has been attributed to the effects of hydrothermal activity (Caratori Tontini et al., this issue). The anomaly encompasses an oblate shaped area up to 2 km long and 1 km wide that begins just offshore the boat jetty (Fig. 4B), and which strikes ~035° towards the north shore of the lake (Fig. 16A). This area in general, and the most negative part of the anomaly in particular, strongly correlate with zones of high heat

flux (Fig. 16B; see Tivey et al., this issue), CO_2 flux (Fig. 16C; see Mazot et al., 2014) and a high density of bubble plumes and hot water discharge (Fig. 16D; see Walker et al., this issue). This is the general area of the pre-1886 Pink Terraces hydrothermal system, with the Pink Terraces per se located towards the northern part of this magnetic anomaly, offshore Otukapuarangi Bay (see Figs. 1 and 4B, and de Ronde et al., this issue). Given that the large Rotomahana Crater was formed only 125 years prior to the survey in 2011, our experience (e.g., Caratori Tontini et al., 2012) shows that insufficient time will have elapsed to enable hydrothermal fluids since that time to have destroyed the magnetite in the volcanic rocks. Thus, the magnetic anomaly largely depicts the upflow zone of the Pink Terraces hydrothermal system *before* the 1886 eruption. Moreover, the high heat flux, CO_2 flux, density of bubble plumes and discharge of hot water in this same area attests to this hydrothermal system having survived the eruption and indeed, continues to be very active today.

Basaltic dikes were observed in the large Rotomahana Crater immediately after the eruption, before they were concealed by rapidly rising lake levels (see Keam, this issue). Certainly, a number of workers have described their occurrence in the rift crater walls of Mt. Tarawera (e.g., Nairn and Cole, 1981) and, by inference, elsewhere along the rift as determined by geophysics (e.g., Rogan and Hochstein, 1984). Outlined in Figure 16A are the magnetic anomalies attributed by Caratori Tontini et al. (this issue) to basalts, based on the amplitude of the magnetic signal. Four of these occurrences are on the northern shore of the lake, one on the western side, and one in the southwest corner of the lake. One of these occurrences correlates to a basaltic outcrop east of Star Hill Crater and another to the Pinnacle. The one on the western shore of the lake correlate with high heat and CO_2 flux measurements and they, together with the Pinnacle occurrence, the 'bubble rock' occurrence further to the east

and the occurrence on the southwest shore of the lake, are associated with noticeable bubble plumes. Only the most northeastern basalt occurrence is not obviously related to these other anomalies, although the bubble plume survey at least did not cover this part of the lake (see Fig. 9C). We believe that these magnetic anomalies are probably related to basaltic dikes of the 1886 eruption. However, that the dikes might still be degassing and/or dissipating heat 125 years after their emplacement is considered unlikely, given their narrow (few m) widths. Rather, they are possibly acting as competency contrasts to the host rocks, providing pathways (permeability) for gases and heat to rise to the lakefloor from below.

Heat flow through the floor of Lake Rotomahana is concentrated in two areas; the western margin of the lake (i.e., the aforementioned Pink Terraces hydrothermal system) and another, distinct area southwest of Patiti Island. A wider area of much lower heat flux occurs over the whole Rotomahana Basin (Fig. 16B). At the southern-most extension of the Pink Terraces hydrothermal system, a 'bulls eye' pattern marking the highest measured heat flux (Tivey et al., this issue) is centered on the most negative magnetic anomaly (Caratori Tontini et al., this issue), where the highest temperature vent fluids were recorded (Walker et al., this issue), bubble plumes are typically very strong (Fig. 15) and the CO_2 flux is also high (Mazot et al., 2014). A donut-shaped pattern of low heat flux around this area possibly marks recharge by ambient lake water. This area, where miniature temperature recorders were deployed on a mooring (Walker et al., this issue), is located above the intersection between the sediment-filled Rotomahana Basin and the sloping western boundary of the inferred Okataina Caldera margin (Nairn, 2002; cf. Fig. 13).

The other area of distinct heat flux shown in Figure 16B is comprised of one dominant and two subordinate 'bull eyes' of high W/m^2 values that together form a

cluster between Patiti Island and the southwestern lakeshore as part of the Patiti hydrothermal system. Strong correlations between heat flux, bubble plumes and hot water discharge in the area is indicative of modern hydrothermal activity. The absence of any correlation with a negative magnetic anomaly is testament to the young age of this hydrothermal system. The correlation with CO_2 flux is not as apparent for this area of high heat flux, likely because this area is covered by 60-90 m of water with the presence of a strong thermocline. This means there is a greater opportunity for CO_2 from the bubble plumes to dissolve as they ascend through the hypolimnion and try to breach the thermocline on their way to the surface. Indeed, Mazot et al. (2014) estimate 90-95% of the CO_2 is dissolved in the lake water below the thermocline, and that there is ~39,000 tonnes of CO_2 trapped in the lake. Also, cooling and vertical mixing create an isothermal water column once a year during the winter months (June through August), while a thermally stratified water column forms from September through May (Walker et al., this issue). As the survey of Mazot et al. (2014) was done between the months of February and April, possibly a very different picture would emerge if the same study was done during the winter, when the lake is not stratified.

Finally, there is an extensive, albeit low-level heat flux anomaly covering the entire Rotomahana Basin (Fig. 16B; see Tivey et al., this issue), with a seismic section through this area suggestive of gas pockets occurring beneath the lakefloor (Fig. 13B). Here, there are no, or very few, recorded instances of bubble plumes (Fig. 15). However, in contrast to the areas of the Pink Terraces and Patiti hydrothermal systems, the lakefloor in the center of the lake is typically deeper than 90 m (Fig. 4A). Thus, any bubbles would have to rise the furthest from the lake floor and would largely dissolve in the water column before reaching the surface. As CO_2 flux at the

surface of the lake is less efficient by diffusion than via bubbles, it is perhaps not surprising that high levels of CO_2 flux on the western side of the lake is coincident with shallow (<60 m) depths and an abundance of bubble plumes that pass through the thermocline.

Aside from the most concentrated area of CO_2 flux associated with the Pink Terraces hydrothermal system, relatively high levels of CO_2 flux are recorded throughout the lake and are typically associated with bubble plumes, such as those related to the Pinnacle area, the bubble rock area, the larger craters just northeast of Patiti Island, the smaller craters further northeast again and an area on the southern-most shore of the lake (Figs. 16C and D). The area of high CO_2 flux southeast of Patiti Island was not covered by the bubble plume survey (Fig. 9C).

The distribution of bubble plumes throughout the lake can be divided into regions (color-coded in Fig. 16D) that are typically related to known hydrothermal, geological and/or geophysical anomalies. For example, the southern-most bubble plumes related to the Patiti hydrothermal system, extend northeastwards from a postulated basaltic dike near the southwest shoreline of the lake (Fig. 16A) and could be related to an extension of this dike. These same plumes also demarcate the steep southern margin of the Rotohamana Crater, where the flank of the crater meets the margin of the Rotomahana Basin (e.g., see Fig. 14); where underlain by sediments of the Rotomahana Basin extensive pockmarks are clearly seen on the lakefloor (Figs. 5A and 12D). By contrast, the southern-most bubble plumes related to the Patiti hydrothermal system are underlain by a large fan delta where pockmarks are less obvious (Fig. 5B), possibly as this environment is constantly changing as new sediment enters the lake and cascades down the fan. The plumes of the Patiti hydrothermal system as a whole form a zone subparallel in strike to the orientation of

the main Rotohamana Crater (see below), inferring a linear control in permeability in this part of the lake. Two possible subparallel trends of bubble plumes are seen in this data, separated at their southwestern end by the aforementioned dike, and may delineate subparallel permeable structures in the sublakefloor. Elsewhere, bubbles are associated with other inferred basaltic dikes (see above), some craters, and the Pinnacle.

Four of five confirmed areas of discharging hot water on the lake floor are strongly associated with bubble plume areas, as is one area of inferred hot water (Fig. 16D). Not surprisingly, the whole Pink Terraces hydrothermal system has significant hot water discharge immediately east of the shoreline, and in another area slightly further eastwards from Otukapuarangi Bay, in the vicinity of the inferred site of the Pink Terraces (de Ronde et al., this issue); both areas are associated with high heat flux. The mooring area also has significant hot water discharge (Walker et al., this issue) and is associated with a separate area of high heat flux. A fifth area of confirmed hot water discharge but with no associated bubble plumes occurs in the northwestern part of the lake (Fig. 16D). However, this area correlates with an extension of the Pink Terraces hydrothermal system magnetic, heat flux and CO_2 flux anomalies (Figs. 16A, B and C) and is coincident with an inferred basaltic dike. Inspection of the bubble survey tracks (Fig. 9C) shows that most of this area was not covered by the survey, thus it is possible some bubble plumes may exist here.

Interpretation of seismic reflection lines

Seismic reflection lines acquired in Lake Rotomahana image the near-surface (< 200 m depth) 1886 Tarawera Linear Vent Zone. Most of the shallow 2-D seismic reflection profiles that were collected are oriented either parallel, or normal, to the

trend of the lake. Along the axis of the lake, seismic lines image sub-horizontal sediments up to 37 m thick resting on an irregular reflector (e.g., Fig. 13). In the two sub-craters that underlie the main Rotomahana Basin, i.e., West Rotomahana Crater and East Rotomahana Crater (and to a lesser extent the Rotomakariri and Waingongongongo Craters), this reflector represents a modification of pre-eruption topography, and is thus considered to represent the post-1886 eruption surface. Elsewhere in the lake, such as the 'high ground' between East Rotomahana Crater and Waingongongongo Crater (see Fig. 13), the bathymetry could represent 1315 AD Kaharoa eruption domes, or even older units, given the diversity of volcanics and their ages, distributed around Lake Rotomahana today (Nairn, 2002). Discontinuous reflectors have also been observed beneath the aforementioned irregular post-1886 surface in a couple of profiles, however, these have not been studied here.

The seismic surveys also aid in locating the western 'topographic' margin of the Okataina Caldera in Lake Rotomahana. That is, seismic sections oriented orthogonal to the strike of the caldera, such as that shown for Line 100 in Figure 13, show that the caldera rim is located ~500 m further to the west than that depicted on the map of Nairn (2002; see Fig. 1A).

The total volume of the Rotomahana Crater was calculated in order to estimate the volume of material ejected during the eruption An isopach map constructed from seismic lines for sub-horizontal sediments confirms the presence of four depressions, or craters, beneath the lake (cf. Fig. 13) that are filled with sediment up to 37 m thick (Fig. 17A). Volumes for the craters were calculated in ArcGIS using a surface volume tool with crater isopachs calculated using a velocity of 1600 m/s and a plane height equal to zero (i.e., equivalent to the present lakefloor). We derived the volume estimates for the four craters as follows: West Rotomahana Crater = 0.006991 km^3;

East Rotomahana Crater = 0.012851 km^3; Waingongongongo Crater = 0.000673 km^3; and Rotomakariri Crater = 0.002123 km^3, for a total volume of sediment infilling the craters of 0.026771 km^3. Using the volume tool in Feldermaus®, where the bathymetry of Lake Rotomahana marks the 'mid-point' boundary of the Rotomahana Crater and the lake surface the upper boundary, we calculate a volume of 0.505730 km^3. This approach seems reasonable considering the general shape of the lake today when compared to Rotomahana Crater in the map made by Smith (1887) immediately after the eruption, together with the various seismic sections showing the northern and southern boundaries of the lake are bounded by relatively steep sided margins (e.g., Fig. 14). However, this volume is most likely a minimum, as some of the craters on the margins of the lake, such as Star Hill Crater and Donne Crater, extend skywards from the surface of the lake. Nevertheless, if we then add the volume calculated from the isopach map of Figure 17A for the portion of the craters buried by sediment, we derive a total volume of 0.5325 km^3 for material ejected from Rotomahana Crater during the 1886 eruption. This value is remarkably similar to the total volume of Rotomahana Mud of 0.529 km^3 mapped around the lake environs by May et al. (this issue).

The depressions depicted by the isopach map have a similar geometry to eruption craters on the summit of Mt. Tarawera (Nairn and Cole, 1981) and in the Waimangu geothermal area immediately southwest of the lake (Simmons et al., 1993). The seismically imaged craters have moderately dipping sides (15-25°) and are generally elongate parallel to the strike of the lake (Fig. 17B). The craters define the linear vent zone beneath the lake where they form a northeast-trending array co-axial with the fissure on Mt Tarawera to the northeast, and the alignment of Donne Crater and the Waimangu craters to the southwest along the same 057° strike. In addition, the 1886

basalt dike planes exposed within the rift crater walls along Mt. Tarawera are oriented at a clockwise direction rotation of ~15° relative to the aforementioned rift direction (Nairn, and Cole, 1981), which is the same angle between the strike of the two Rotomahana craters and a line drawn between the centers of these craters, coincident with the saddle that separates the craters (Fig. 17A). If this saddle were to represent an area of basaltic dike intrusion, it would not be recognized in the magnetic survey due to the narrow width of the dike (~2 m) combined with the depth of water (118 m) and thickness of sediment (~20 m) covering the saddle.

In detail, the vent system beneath the lake forms an array of right-stepping (dextral) craters. The general trend and segmentation of the vent system may reflect the strike and segmentation of the underlying dikes formed during the 1886 eruption. Diking requires an extensional regime. The right-stepping vent geometry could be interpreted to indicate mainly extension with a small component of right-lateral shear across the lake, however, kinematic data from GPS, historical earthquakes and geological mapping (Seebeck et al., 2014) indicate that the present extension direction (145° N) is approximately perpendicular to the trend of the vent system. The parallelism of linear vents, dike(s) and rift faults is consistent with a model in which far-field tectonic stresses (e.g., Wallace et al., 2004) strongly influence the northwest-southeast extension direction reprsented by faulting and dike intrusion. Calculation of the ratio of maximum crater diameter to crater 'depth', as defined by the isopach map in Figure 17A, shows the four largest craters, i.e., Rotomhana West, Rotomahana East, Waingongongo and Rotomakarii have values of 20, 27, 28 and 20, respectively. These values are relatively consistent and are noticeably higher than the typical value of ~5 for the craters on the margin of the lake (see Table 1). This reflects the broader and relatively shallower nature of the craters buried along the axis of the lake, which

we interpret to reflect relatively more explosive phreatomagmatic eruptions considering these craters formed largely beneath old Lake Rotomahana.

Evolution of the Waimangu-Rotomahana hydrothermal system

The well-documented sequence of events pertaining to the 1886 eruption of Mt. Tarawera culminated in a paroxysmal phreatomagmatic eruption in the Lake Rotomahana area (Keam, 1988). Most of the present-day lake fills the Rotomahana Crater mapped by S. Percy Smith—and not just that part filled by sediment beneath the lakefloor—which he described as a "…circular basin-shaped hollow 2.5 km in diameter surrounded by precipitous slopes and in some places vertical cliffs varying from 60 to nearly 100 m in height and cored out near its center to a greatest depth of ~160 m (Smith, 1887, pp. 55-56, as quoted in Keam, this issue). Here, we have been able to reconstruct the Rotomahana Crater and find the dimensions remarkably similar to those stated by Smith (1887) with the nearly circular, main body of the lake indeed 2.5 km in diameter and the calculated depth to the bottom of the crater of 155 m. In concert with the magnitude of excavation of Lake Rotomahana during the phreatomagmatic eruption of 1886, altered rhyolite and ignimbrite lithics were common in the study of the Rotomahana Pyroclastics unit by Pittari et al. (this issue), confirming the occurrence of a significant volume of hydrothermally altered rock in the Rotomahana area prior to the eruption. These authors suggest that the diversity in lithic types indicate a spatial variation in country rock lithology and strength that may have contributed to the location and morphology of the craters beneath Lake Rotomahana.

Gravity modeling by Seebeck et al. (2010) shows that the TVLS, which extends from Mt. Tarawera to Waimangu (Nairn et al., 2002), occurs vertically above the

intersection of the southeastern caldera structural margin and the inferred caldera floor. Thus, the basaltic dikes that were the focus of the 1886 eruption have a fairly deep-seated origin. Moreover, it has been suggested by Rowland et al. (2010) that mafic diking from 'source to surface' along length-scale features such as the TLVZ provide compelling evidence that 'magma-assisted' rifting in the form of dike intrusion can be an important extension mechanism within the central part of the Taupo Volcanic Zone.

The Pink (and White) Terraces hydrothermal system was obviously active prior to the 1886 eruption, with suggestion that it is at least several hundred years old (Keam, this issue) and the focus of fluid upflow in the vicinity of the old Lake Rotomahana before the 1886 eruption. However, the high-resolution magnetic survey of the lake, when combined with regional airborne magnetic data, clearly shows a negative anomaly associated with the Pink Terraces hydrothermal system and that it extends southwestwards beneath the present-day Waimangu geothermal system (Caratori Tontini et al., this issue). This is consistent with the modern resistivity map of the area, which shows the 20 Ω m contour clearly encompassing both hydrothermal areas (Stagpoole and Bibby, 1998). While no evidence was found for surface discharge of hydrothermal fluids at Waimangu before 1886, the extent of the aforementioned geophysical boundaries combined with similarly hydrothermally altered ejecta in the area (Keam, this issue; Simmons et al., 1993) suggest that a buried hydrothermal system existed in this area. The effect of the 1886 eruption in the Waimangu area was therefore most likely phreatic activity associated with an existing hydrothermal system.

The old Pink and White Terraces likely sat eastwards of the Okataina Caldera rim prior to the eruption of 1886, consistent with the location of the caldera rim

determined in this study and the majority of the area defined by the Pink Terraces hydrothermal system negative magnetic anomaly (Figs. 13B and 16A). Thus, the caldera margin may have acted as a significant pathway for the ascent of hydrothermal fluids. Today, significant amounts of gases are being expelled into Lake Rotomahana. The annual geothermal output of CO_2 into Lake Rotomahana is greater per unit surface area (for the lake alone) than seen at other geothermal systems in the Taupo Volcanic Zone (Fig. 18). Such high levels of CO_2 can only be ascribed to the degassing of a relatively shallow magma body in the region. This is consistent with the lake being supersaturated with respect to ^3He (Stucker et al., this issue).

The presence of a relatively shallow magma chamber beneath Lake Rotomahana, or in the near vicinity, is corroborated by a recent study by Heise et al. (this issue) who analyzed broadband magnetotelluric (MT) data, targeting the heat source and upflow zones beneath the area in an attempt to examine the deeper magmatic sources beneath this region. Results from 3-D inversion of the MT data show the Waimangu area— extending over to the western side of Lake Rotomahana—is underlain by a relatively shallow (~500 m) zone of low resistivity clay (smectite-dominated) hydrothermal alteration, that is in turn underlain by a deeper (~500-3000 m) zone of higher temperature, higher resistivity illite-dominated alteration. These alteration zones are in turn fed by a high-temperature, highly conductive up-flow zone emanating from the northeastern edge of a deep source, rising beneath Frying Pan and Okaro lakes of Waimangu, and the western part of Lake Rotomahana. Heise et al. (this issue) describe this up-flow zone as quasi-magmatic fluid that ascends from ~8 km depth to within ~3.5 km of the surface. These authors infer a melt fraction of between 8 and 23% for the deeper part of the conductive zone, and on the basis of the

resistivity values, infer the presence of hyper-saline liquid surrounding the underlying body of crystallizing silicic magma.

In another study, earthquake relocation analysis of 913 earthquakes recorded in the area between 2004 and 2015 show an earthquake cluster near Waimangu-Rotomahana, where seismic activity largely occurs along a single ~7 km long NE-SW fault lineation, with individual bursts of seismic activity on isolated areas on that fault (Bannister et al., this issue). The fault is an active sub-surface fault that extends along the northern side of Waimangu geothermal system towards the northwestern end of Lake Rotomahana, and correlates with the highly conductive up-flow zone of Heise et al. (this issue). This fault is therefore considered a prime candidate for a permeable pathway enabling the upflow of magmatic gases (e.g., CO_2 and ^3He) to the Pink Terraces hydrothermal field (cf. Bannister et al., this issue). Moreover, this fault may explain the high heat flow on the western side of Lake Rotomahana (Tivey et al., this issue) and the periodic release of hot water recorded on the lakefloor by our instruments (Walker et al., this issue). The modern Patiti hydrothermal system in the southern part of Lake Rotomahana likely utilizes structures related to the Rotomahana Craters for hydrothermal fluid (including gas) flow to the lakefloor.

In summary, the Pink Terraces and Patiti hydrothermal systems of Lake Rotomahana have their heat and gases derive from a nearby magma chamber that is likely responsible for hydrothermal activity in the Waimangu-Rotomahana areas both before, and subsequent to, the 1886 eruption of Mt. Tarawera. However, it is unclear if this magma body is responsible for the emplacement of the basaltic dikes along the Rotomahana Crater. Either way, a significant heat source is available to fuel geothermal systems in the area for the foreseeable future. Application of state-of-the art bathymetric mapping and seismic surveys has enabled us to reconstruct the

geology and structure of the main Rotomahana Crater and subsidiary craters to the northwest, effectively removing the water column of Lake Rotomahana and 125 years of infill sediments. This has provided an unencumbered context for the eruption of June 10 1886 and it effects on the Pink and White Terraces hydrothermal systems, and relationship to nearby vents of Mt. Tarawera and Waimangu (Fig. 19).

Acknowledgements

We gratefully acknowledge iXSurvey for providing in-kind assistance in the acquisition of multi-beam data for this project, and Dave Mundy and Mark Matthews for their expertise in doing an excellent job of surveying Lake Rotomahana. Dirk Immenga of the University of Waikato provided expert boatsmanship and safe working conditions during the seismic survey, camera and CTDO deployments. We thank Steve Wilcox (NIWA) for acquisition of the Boomer seismic data. We also acknowledge the Te Arawa Lakes Trust Board for providing access to the lake and for their ongoing encouragement to do this research. Harvey James and all the team at Waimangu Volcanic Valley were instrumental in providing safe and regular access to the lake. The Rotorua Lakes District Council provided access to the aerial photographs used in Figure 19. Heidi Berkenbosch is thanked for her help in creating some of the figures. C de R would like to acknowledge valuable discussions with Ron Keam (U. of Auckland) and help provided by Rawiri Faulkner (GNS) in making this project a reality. This is PMEL contribution number 4352. Funding for this project was by way of the GNS Science Strategic Development Fund.

References

Bannister, S., Sherburn, S. and Bourguignon, S, 2015, Earthquake swarm activity

highlights a crustal fault associated with the Waimangu-Rotomahana - Mt Tarawera geothermal field, Taupo Volcanic Zone, New Zealand. *J. Volcanolog. Geotherm. Res.*, this issue.

Bloomberg, S., Werner, C., Rissmann, C., Mazot, A., Horton, T., Gravley, D., Kennedy, B. and Oze, C., 2014, Soil CO_2 emissions as a proxy for heat and mass flow assessment, Taupo Volcanic Zone, New Zealand. *Geochem. Geophys. Geosyst.* **15**, doi:10.1002/2014GC005327.

Caratori Tontini, F., Davy, B.W., de Ronde, C.E.J., Embley, R.W., Leybourne, M. and Tivey, M.A., 2012, Crustal magnetization of Brothers volcano, New Zealand, measured by autonomous underwater vehicles: geophysical expression of a submarine hydrothermal system. *Econ. Geol.* **107**, 1571-1581.

Caratori Tontini, F., de Ronde, C.E.J., Scott, B.J, Soengkono, S. Stagpoole, V., Timm, C. and Tivey, M.A., 2015, Interpretation of gravity and magnetic anomalies at Lake Rotomahana: geological and hydrothermal implications. *J. Volcanol. Geotherm. Res.*, this issue.

Christenson, B.W., Mazot, A. and Britten. K., 2010, Gas transfer through Ruapehu crater lake: Insights gained from a recent water-borne survey. Abstract V23A-2388, 2010 Fall Meeting, AGU, San Francisco, Calif., 13-17 Dec. 2010.

Cole, J.W., 1973, High-alumina basalts of Taupo Volcanic Zone, New Zealand. *Lithos* **6**, 53-64.

Crane, K., Hecker, B. and Golubev, V., 1991, Hydrothermal vents in Lake Baikal. *Nature* **350**, 281.

Davy, B. and Bibby, H., 2005, Seismic reflection imaging of the Haraharo Caldera boundary beneath Lake Tarawera, Okataina Volcanic Centre, New Zealand, *New Zealand Journal Geol. Geophys.* **48**, 153-166.

de Ronde, C.E.J., Stoffers, P., Garbe-Schönberg, D., Christenson, B.W., Jones, B., Manconi, R., Browne, P.R.L., Hissmann, K. Botz, R., Davy, B.W., Schmitt, M. and Battershill, C.N., 2002, Discovery of active hydrothermal venting in Lake Taupo, New Zealand. *J. Volcanol. Geotherm. Res.* **115**, 255-273.

de Ronde, C.E.J. et al., 2015, The Pink and White Terraces of Lake Rotomahana: Did they survive the 1886 eruption of Mt. Tarawera? *J. Volcanol. Geotherm.* (this issue).

de Ronde, C.E.J. and Scott, B.J., 2015, Introduction to the special issue "Evolution of the sublacustrine geothermal system of Lake Rotomahana, New Zealand: Effects of the 1886 Mt. Tarawera eruption". *J. Volcanol. Geotherm.* (this issue).

Dymond, J., Collier, R.W. and Watwood, M.E., 1989, Bacterial mats from Crater Lake, Oregon and their relationship to possible deep-lake hydrothermal venting. *Nature* **342**, 673-675.

Heise, W., Caldwell, T.G. Bertrand, E.A., Hill, G.J., Bennie, S.L. and Palmer, N.G., 2015, Imaging the deep source of the Rotorua and Waimangu geothermal fields, Taupo Volcanic Zone, New Zealand. *J. Volcanol. Geotherm. Res.*, this issue.

Hochstetter, F. von, 1864. [Scherzer, K.R., Geologischer Theil Erster Band: Erste Abtheilung, Geologie von Neu-Seeland…Wein] volume 1 part 1 Geologie von Neu-Seeland. Beitrage zur Geologie der Provinzen Auckland und Nelson von Dr. Ferdinand von Hochstetter, 274 pp.

Houghton, B.F., Wilson, C.J.N., McWilliams, M.O., Lanphere, M.A., Weaver, S.D., Briggs, R.M. and Pringle, M.S., 1995, Chronology and dynamics of a large silicic magmatic system: central Taupo Volcanic Zone. *Geology* **23**, 13-16.

Irwin, J., 1982, Lake Rotomahana bathymetry, 1:10,309. *New Zealand Oceanographic Institute Chart*, Lake Series.

Keam, R.F., 1988, Tarawera: the volcanic eruption of 10 June 1886. R.F. Keam – Auckland, New Zealand. 472 pp.

Keam, R.F., 2015, The Tarawera eruption, Lake Rotomahana, and the origin of the Pink and White Terraces. *J. Volcanolog. Geotherm. Res.*, this issue.

May, M.D., White, J.D., Rosseel, J.-B., Carey, R.J. and Houghton, B.F., 2015, Deposit characteristics and energetics of the maar-forming Rotomahana segment of the Tarawera 1886 eruption, North Island, New Zealand. *J. Volcanolog. Geotherm. Res.*, this issue.

Mazot, A., Schwandner, F.M., Christenson, B., de Ronde, C.E.J., Inguaggiato, S., Scott, B., Graham, D., Britten, K. Keeman, J. and Tan, K., 2014, CO_2 discharge from the bottom of volcanic lake Rotomahana, New Zealand. *Geochem. Geophys. Geosystems* **15**, DOI: 10.1002/2013GC004945.

Muir, S., 2012, Characterising lake-floor sediments and pore fluids of a geothermally active volcanic crater lake, Lake Rotomahana. ERTH311-12A – Special topics in Earth Science report, University of Waikato, 42 pp.

Nairn, I.A. and Cole, J.W., 1981, Basalt dikes in the 1886 Tarawera Rift. *New Zealand J. Geol. Geophys.* **24**, 585-592.

Nairn, I.A., Hedenquist, J.W., Villamor, P., Berryman, K.R. and Shane, P.A., 2005, The ~1315 Tarawera and Waiotapu eruptions, New Zealand: contemporaneous rhyolite and hydrothermal eruptions driven by an arrested basaltic dike system? *Bull. Volcanol.* **67**, 186-193, doi 10.1007/s00445-004-0373-7.

Nicol, A., Walsh, J.J., Berryman, K. and Villamor, P., 2006, Interdependence of fault displacement rates and paleoearthquakes in an active rift. *Geology* **34**, 865-868.

Nicol, A., Walsh, J.J., Villamor, P., Seebeck, H. and Berryman, K.R., 2010, Normal fault interactions, paleoearthquakes and growth in an active rift. *J Structural Geol*. **32**, 1101-1113. DOI:10.1016/j.jsg.2010.06.018.

Pittari A., Briggs R.M. and Bowyer D.A., 2015, Subsurface geology and ancient hydrothermal systems beneath Lake Rotomahana: evidence from lithic clasts of the 1886 AD Rotomahana pyroclastics. *J. Volcanolog. Geotherm. Res.,* this issue.

Remsen, C.C., Val Klump, J., Kaster, J., Paddock, R., Anderson, P. and Maki, J.S., 1990, Hydrothermal springs and gas fumaroles in Yellowstone Lake, Yellowstone National Park, Wyoming. *National Geographic Res*. **6**, 509-515.

Rissmann, C., Christenson, B., Werner, C., Leybourne, M., Cole, J. and Gravley, D., 2012, Surface heat flow and CO_2 emissions within the Ohaaki hydrothermal field, Taupo Volcanic Zone, New Zealand. *Appl. Geochem*. **27**, 223–239, doi:10.1016/j.apgeochem.2011.10.006.

Rogan, M. and Hochstein, M.P., 1984, Magnetic survey of the 1886 Tarawera Rift. *New Zealand J. Geol. Geophy*. **27**, 237-245.

Rowland, J.V., Wilson, C.J.N. and Gravley, D.M., 2010, Spatial and temporal variations in magma-assisted rifting, Taupo Volcanic Zone, New Zealand. *J. Volcanol. Geotherm. Res*. **190**, 89–108, doi:10.1016/j.jvolgeores.2009.05.004

Seebeck, H. and Nicol, A., 2009, Dike intrusion and displacement accumulation at the intersection of the Okataina Volcanic Centre and Paeroa Fault zone, New Zealand. *Tectonophysics* **475**, 575-685, doi:10.1016/j.tecto.2009.07.009.

Seebeck, H., Nicol, A., Stern, T., Bibby, H. and Stagpoole, V., 2010, Fault controls on the geometry and location of the Okataina Caldera, Taupo Volcanic Zone, New Zealand. *J. Volcanol. Geophys. Res*. **190**, 136-151, doi:10.1016/j.jvolgeores.2009.04.011.

Seebeck, H., Nicol, A., Villamor, P., Ristau, J. and Pettinga, J., 2014, Structure and kinematics of the Taupo Rift, New Zealand. *Tectonics* **33**, doi:10.1002/2014TC003569.

Shane, P., Smith, V.C. and I. Nairn, I.A., 2008, Millennial time-scale resolution of rhyolite magma recharge at Tarawera volcano: Insights from quartz chemistry and melt inclusions. *Contrib. Mineral. Petrol.* **156**, 397-411.

Simmons, S.F., Keywood, M., Scott, B.J. and Keam, R.F., 1993, Irreversible change of the Rotomahana-Waimangu hydrothermal system (New-Zealand) as a consequence of a volcanic-eruption. *Geology* **21**, 643-646.

Smith, S.P., 1887, *The Eruption of Tarawera*, New Zealand, George Didsbury, Government Printer, Wellington, 84p. (Note: Title page omits New Zealand and has date as 1886 [incorrect]).

Stagpoole, V. M. and Bibby, H. M., 1998, Electrical resistivity map of the Taupo Volcanic Zone, New Zealand; nominal array spacing 500 m, 1:250 000, version 1.0. Institute of Geological & Nuclear Sciences geophysical map 11. Institute of Geological & Nuclear Sciences Limited, Lower Hutt, New Zealand.

Stucker, V.K., de Ronde, C.E.J., Scott, B.J., Wilson, N.J., Walker, S.L. and Lupton, J.E., 2015 Subaerial and sublacustrine hydrothermal activity at Lake Rotomahana. *J. Volcanolog. Geotherm. Res.*, this issue.

Tiercelin, J.-J., Pflumio, C., Castrec, M., Boulegue, J., Rolet, J., Coussement, C., Stetter, K.O., Huber, R., Buku, S. and Mifundu, W., 1993, Hydrothermal vents in Lake Tanganyika, East African Rift system. *Geology* **21**, 499-502.

Tivey, M.A., de Ronde, C.E.J., Caratori Tontini, F., Walker, S.L. and Fornari, D.J., 2015, A novel heat flux study of a geothermally active lake—Lake Rotomahana, New Zealand. *J. Volcanolog. Geotherm. Res.*, this issue.

Villamor, P. and Berryman, K, 2001, A late Quaternary extension rate in the Taupo Volcanic Zone, New Zealand, derived from fault slip data. *New Zealand J. Geol. Geophys.* **44**, 243-269.

Villamor, P., Berryman, K.R., Nairn, I.A., Wilson, K., Litchfield, N. and Ries, W., 2011, Associations between volcanic eruptions from Okataina volcanic center and surface rupture of nearby active faults, Taupo Rift, New Zealand: Insights into the nature of volcano-tectonic interactions. *Geol. Soc. Am. Bull.* **123**, 1383-1405, doi:10.1130/B30184.1.

Walker, S.L., de Ronde, C.E.J., Fornari, D., Tivey, M.A. and Stucker, V.K., 2015, High-resolution water column survey to identify active sublacustrine hydrothermal discharge zones within Lake Rotomahana, North Island, New Zealand. *J. Volcanolog. Geotherm. Res.*, this issue.

Wallace, L.M., Beavan, J., McCaffrey, R. and Darby, D., 2004, Subduction zone coupling and tectonic block rotations in the North Island, New Zealand. *J Geophys. Res.*, B12406. doi:10.1029/2004JB003241.

Wilson, C.J.N., Gravley, D.M., Leonard, G.S. and Rowland, J.V., 2009, Volcanism in the central Taupo Volcanic Zone, New Zealand: tempo, styles and controls. *In:* T. Thordarson, G. Larsen, S. Self, S. Rowland and A. Hoskuldsson (Eds.) *Studies in Volcanology: The Legacy of George Walker*, (Special Publications of IAVCEI 2, 225–247). London, United Kingdom: Geological Society.

Figure captions

Figure 1. (A) Map of the Okataina Volcanic Center (OVC), including the Okataina Caldera, with the bold dashed lines outlining the erosional margin of successive caldera collapse. Also shown are the most dominant regional faults of the Taupo Fault Zone (lower left-hand side). Figure modified after Shane et al. (2008), Nairn (2002) and Mazot et al. (2014). Inset: Map of the North Island of New Zealand showing the location of the Taupo Volcanic Zone. (B) Location map of Lake Rotomahana showing the location of the pre-1886 lakes Rotomahana and Rotomakariri (dark blue), superimposed on the modern lake area (light blue; modified from Nairn, 2002; old Lake Rotomahana outline taken from Keam, this issue); asterisks mark the location of the Pink and White Terraces with respect to pre-1886 Lake Rotomahana.

Figure 2. Photographs of the geology around the lake margin. A. Cross-bedded, pyroclastic surge deposit considered to be between 28 and 22 ka in age (Nairn, 2002). B. Rhyolite lava seen outcropping on the western side of Patiti Island that has been ascribed an age of 18 ka as part of the Okareka eruptive episode (Nairn, 2002). C. Prominent headland (otherwise known as 'Green Lake plug') that separates Green Lake Crater from Lake Rotomahana in the very northeastern end of the lake, and is related to the ~1314 AD Kaharoa eruptive episode (Nairn, 2002). D. A cut on Waimangu Valley Road was exposed during the 2011 field season. Subject is pointing to the base of the Rotomahana mud that was expelled during the June 10 1886 eruption. The black horizon marks the paleosol buried by the mud.

Figure 3. Hydrothermal manifestations seen along the margin of Lake Rotomahana. A. Steaming Cliffs on the far western side of the lake at the margin to Donne Crater with hot springs near the water's edge. B. Fumaroles along the western shoreline of the

lake, this time along Awarua Cliffs in Fumarole Bay. C. Miniature geysers seen along the western shoreline, commonly occurring within a few m of the lake level, base of Donne Cliffs. D. Locally known as "Angel Wings" geyser on the western margin of Donne Crater (see Stucker et al. and Walker et al., this issue), this spectacular feature was regularly spouting hot water during 2011 when the lake level rose to its highest level, but which has since become more subdued and has had one of its 'wings' break off. Note the small, boiling spring to the right just above the lake level, and the surrounds, which show prevalent coatings of silica. E. The prominent Otukapuarangi Bay Geyser that occurs along the northern section of the western shoreline (see Stucker et al., this issue) erupts every ~20 minutes and reaches heights of ~7-8 m when in full flight (not shown). F. Example of bubble plumes that rise from the lakefloor to the lake surface (Bubble Rock area), seen commonly throughout Lake Rotomahana (see Fig. 15 later). See Figure 4B for position of locations noted above.

Figure 4. A. High-resolution (0.5 m) bathymetric map of 8.9 km^2 Lake Rotomahana. Total duration of actual data logging during the survey was 10 hours and 25 minutes. The total area surveyed was 14.6 km^2, which includes significant overlap acorss the swaths. A number of sedimentary basins and volcanic features are clearly prominent in the map (see text for details). Projection is WGS84, UTM zone 60S. B. Line drawing interpretation of the bathymetric map shown in (A). The lake is dominated by the Rotomahana Basin, which is up to 118 m below lake level, sedimentary fan deltas, and volcanic craters (see text for details).

Figure 5. Select features of Lake Rotomahana bathymetry (see Fig. 4B for locations).

A. Large zone of pockmarks formed by discharging gas, southern side of Rotomahana Basin. B. Sediment fan delta extending into the lake from the shallow swampy area in the south. C. Prominent, arcuate-shaped ridges in the vicinity of the pre-1886 Pink Terraces. D. Cluster of small craters NE of Patiti Island formed within the general confines of the Rotomahana Crater. E. Pefectly formed maar eruption crater, hereafter called Smith Crater after S. Percy Smith who surveyed the Rotomahana Crater immediately after the eruption in July 1886. F. Clearly demarcated 'wave cut' terraces on the margin of the lake that likely represent earlier (older) lake levels. See Figure 4B for locations.

Figure 6. Pinnacle area (see Fig. 4B for location). A. Painting made by Charles Blomfield in October 1886 of what has been coined "The Pinnacle", thought to be a dike that occupies part of what was Pinnacle Ridge, near the site of the White Terraces (see Keam, this issue). B. High-resolution (0.5 m) bathymetry showing a 3D view of the same Pinnacle with remarkable detail. Mt. Tarawera is seen in the background in both the painting and in the digital terrain map (grey) laid on top of the bathymetric data.

Figure 7. Star Hill Crater (see Fig. 4B). A. Photograph taken by Burton Bros in late July / early August 1886. B. High-resolution (0.5 m) bathymetry with digital terrain overlain that shows the bottom half of the crater in detail, even showing remnant pockmarks that likely mark the location of fumaroles shown in the photograph (lower right-hand side).

Figure 8. Submerged lake levels taken from select profiles around the margin of

Lake Rotomahana, representative of hiatus events in the filling of the lake. Terrace 'h' and/or Terrace 'g' are similar in height above sea level, and possibly represent the maximum height of Greater Lake Tarawera that would have also encompassed Lake Rotomahana.

Figure 9. Location of surveys done on Lake Rotomahana. A. Camera deployments have been labeled consecutively for both field seasons, thus the 2011 camera lowerings are numbered 1-16 and those for 2014, 17-34. For location of conductivity-temperature-depth-optical (CDTO) casts, see Walker et al. (this issue). B. Seismic survey lines covered during this study. Line 100 is shown in Figure 13 and Lines 303 and 500b in Figure 14. M, mooring. Inset shows high-density line spacing over the area where the Pink Terraces are considered to have stood (see de Ronde et al., this issue). C. High density spacing of the bubble plume survey.

Figure 10. Photographs of sub-lacustrine sediments in Lake Rotomahana. A. Image covering ~1.5 m across of the lakefloor away from the steep bathymetry that mostly surrounds the lake (camera deployment 2011_Cam-16; see Fig. 9A). The lighter colored material is organic flocculent that sits on top of a darker, carbonaceous-rich unit (see 10C and 10D). B. Similar material as seen in (A) only here distinct ripples can be seen on the lakefloor (2011_Cam-13; image ~1.5 m across). C. Close-up photo of the orange-yellow flocculent material that covers much of the lakefloor and which is host to plant matter, the occasional (probable chironomid) worm together with burrows and other bioturbation features. Cylinder is ~8 cm in diameter. Core sample was collected ~500 m E of the Awarua cliffs (Muir, 2012). D. A black, organic-rich unit sits directly beneath the flocculent material, which in turn is

underlain by gray colored, finer grained sediment that is considered to be Rotomahana Mud, or part of the Tarawera Tephra deposited from the 1886 eruption. Core collected offshore of Fumarole Bay, about ~125 m E of the shoreline (Muir, 2012; see Pittari et al., this issue?).

Figure 11. Photographs of sub-lacustrine geology within Lake Rotomahana. A. Looking down on a rough-textured surface unit that is typically massive although locally shows crude layering and which is host to numerous clasts, thought to represent the Rotomahana Mud (camera deployment 2014_Cam-26). View is ~2.5 m across. B. Similar material to that shown in (A) although locally can be covered by organic material (top right; cf. Fig. 10D) with clasts also present (2014_Cam-29). View is ~1.5 m across. C. Layered ash units (2014_Cam-29). View is ~2.5 m across. D. More layered, probable Rotomahana Mud material that locally shows evidence for hydrothermal alteration in the matrix to larger, embedded blocks (center right-hand side; 2014_Cam-22). View is ~2 m across. E. Unit of unaltered, probable Rotomahana Mud (left-hand side), sitting on top of a unit that appears to be extensively hydrothermally altered (2014_Cam-20). View is ~2.5 m across. F. Large hydrothermally altered blocks (e.g., centre left) set in what appears to be a finer-grained matrix where hydrothermal alteration is prominent (2014_Cam-24). View is ~3 m across. G. Another example of a large volcanic block either set within, or has draped overtop, mud like material (2014_Cam-25). Note the probable kōaro (*Galaxias brevipinnis*) fish in the foreground. View is ~1.5 m across. H. A rare example of massive blocks of lava from the Pinnacle area (2011_Cam-7). View is ~2 m across. For location of camera stations, see Figure 9A.

Figure 12. Photographs of sub-lacustrine hydrothermal activity in Lake Rotomahana. A. Example of gas bubbles being discharged from a pockmark on the lake floor in an area NE of Patiri Island. Camera deployment 2014_Cam-29. View is ~2 m across. B. Example of hot water being expelled from a pair of vents near the Pinnacle area, as seen by the shimmering water on the left-hand side of the larger vent (2014_Cam-25; view is ~1 m across). Hot water was detected in several places within the lake (see Walker et al., this issue). C. In the southwestern part of the lake, where the heat flow is highest (see Tivey et al., this issue) and near where the mooring was deployed (area 'D' of Walker et al., this issue; see Fig. 16B later), there is a high density of pockmarks that are discharging gas and/or hot water (2014_Cam-31; view is ~2 m across). D. In contrast to (C), the newly formed vents, or pockmarks, found in the Patiti hydrothermal system area on the southern margin of Rotomahana Crater (see Figs. 5A, 14 and 15 later) can commonly reach sizes of ≥1 m in diameter. Brown material in foreground is flocculent disturbed off the bottom by the camera (2011_Cam-9; view is ~1 m across). E. Relatively massive unit in the Pinnacle area that has a crust on its outer surface, which is in turn underlain by yellow and white colored, hydrothermally altered material (2014_Cam-26; view is ~1.5 m across). F. Example of large-scale hydrothermal alteration of a volcanic unit that is in part layered but elsewhere appears to contain various blocks of material (2014_Cam-26; view is ~1.5 m across). G. Example of a crust near a crater NE of Patiti Island that is surrounded by hydrothermally altered material that includes some hieroglyphics-like textures (2014_Cam-30; view is ~2 m across). H. Another unusual pattern seen in a similar area near (G) that resembles Maori motifs; it is uncertain if this can be attributed to hydrothermal alteration or possible liesegang weathering before the lake rose (2014_Cam-29; view is ~2.5 m across). For location of camera stations, see

Figure 9A.

Figure 13. Seismic section along the length of Lake Rotomahana (see Fig. 9B for line location). A. Processed seismic data showing the prominent Okataina Caldera rim bounding two sediment-filled sub-basins comprising the Rotomahana Basin in the southwestern end of the section and the smaller Hochstetter, Waingongongongo and Rotomakariri Basins at the northeastern end of the section, respectively, with intervening volcanic 'highs'. Pockets of gas are noticeable in the Rotomahana Basin in particular. B. Interpretation of the lakefloor (blue line) and volcanic 'basement' (red line) beneath the sediments thought to represent the post-1886 eruption surface. The intersection of seismic Lines 500b and 300 are shown for reference (see Fig. 14).

Figure 14. Seismic sections across Lake Rotomahana (see Fig. 9B for line locations). Both sections (A and B; C and D) clearly show the relatively steep margins of the explosion crater with sediment infilling the deepest parts. Line 303 shows more clearly other volcanic features near the SE end of the line. The intersection of Line 100 is shown for reference (see Fig. 13). Interpreted horizons are as in Figure 13.

Figure 15. Bubble plume survey of Lake Rotomahana overlain on gray-scale high-resolution bathymetry. Two areas predominate the distribution pattern of the plumes; one at the western end of the lake (i.e., the old Pink Terraces geothermal area), and the other striking ENE from the southwestern shoreline to Patiti Island (i.e., the southern margin of Rotomahana Crater). Each of the five categories of plume types plotted in the figure and mentioned in the text are shown below the map, with examples photographed from the sounder.

Figure 16. Compilation maps from data collected during other surveys, overlain on the high-resolution bathymetry. A. Magnetic data reveals a pronounced negative anomaly depicting hydrothermal activity of the Pink Terraces hydrothermal system on the western side of the lake. Bold dashed lines outline inferred basaltic dikes (see Caratori Tontini et al., this issue). B. Heat flux data that correlate with the Pink Terraces hydrothermal system but which also mark the post-1886 Patiti hydrothermal system in the southern part of the lake and to a lesser extent, the Rotomahana Basin as a whole (see Tivey et al., this issue). C. CO_2 flux data shows correlation with both hydrothermal systems and the aforementioned basaltic dikes. Measurements were made over 10 field campaigns between April 2010 and February 2011, resulting in 484 data points covering the entire lake area (Mazot et al., 2014). This includes measurements taken in April and on five separate occasions in December 2010, and once in January, twice in February and once in March of 2011. Thus, all the measurements were performed when the lake was thermally stratified (cf. Walker et al., this issue). D. Gas and hot water discharge data. Bubble plumes are color coded by location (see text). The majority of bubble plumes are associated with the Pink Terraces and Patiti hydrothermal systems, and to a lesser extent Pinnacle Ridge, some of the inferred basalt dikes, and some small clusters of craters in the NE part of the lake.

Figure 17. A. Sediment isopach map derived from seismic sections (see Fig. 9B) showing the predominant western and eastern sub-basins of the larger Rotomahana Basin, and the lesser Hochstetter, Waingongongo and Rotomakariri Basins in the NE of the lake. Isopach thickness of sediments derived using a velocity of 1600 m/s (see

text). Pink line marks a strike of 057°, or the general orientation of the volcanic vents throughout the region; bright green line strikes 072° (or 15° clockwise from the volcanic vents), which is the reported strike of basaltic dikes seen in the walls of the craters on Mt. Tarawera. B. Oblique view of a 3-D model for the sediment-filled craters of Lake Rotomahana, looking along an azimuth of 035° E. 4 x vertical exaggeration used on the 3D image to highlight the geometry of the craters in two-way travel time (see Figs. 13 and 14).

Figure 18. Plot of measured CO_2 annual flux versus area for select New Zealand geothermal systems and active volcanoes. Lake Rotomahana has the highest flux of CO_2 over the greatest area of all the sites. Data sources are as follows: White Island and Rotokawa (Bloomberg et al., 2014), Ruapehu (Christenson et al., 2010), Ohaaki (Rissmann et al., 2012) and Rotomahana (Mazot et al., 2014).

Figure 19. Aerial photograph showing Mt. Tarawera to the NE and Waimangu to the SW with bathymetry and isopach thickness of Lake Rotomahana superimposed. A line of volcanic vents can clearly be seen extending through all three areas, with the series of craters discussed in this study noticeable within Lake Rotomahana. The isopach data, where >2.5 m in thickness, was brought in separately for each part of the grid (i.e., Rotomahana and 'NE' basins) and color scales set so that the isopach contours appear to be continuations with the depth scale. The areas with 0-2.5 m isopach thickness are broad, and cover more of the bathymetry than is necessary to show in this figure. The 0 m isopach contour in the northeastern end of the lake (Fig. 17A) was consistently ~70 m depth. However, in the main basin, the depth of the 0 m isopach thickness contour ranged from 90 to 115 m.

Appendix I: Methods

Bathymetric survey

The most recent bathymetric survey of Lake Rotomahana was conducted over four days between 28 February and 2 March 2012. We used the purpose built, 7m long multibeam echo-sounder (MBES) survey motor boat *Elaine* of iXSurvey, equipped with a Kongsberg EM3002D (dual head) multibeam echo-sounder coupled with a Trimble SPS851 WADGPS Positioning (OmniStar HP) system and an iXSea ROVINS inertial navigation system; an HP Core Workstation was used as the acquisition computer. A Valeport mini sound velocity sensor was used to acquire velocity profiles of the water column.

All sounding data were recorded when the water level of Lake Rotomahana was between 339.880m and 339.885m above mean sea level (Moturiki Datum 1953; see http://www.linz.govt.nz/data/geodetic-system/datums-projections-and-heights/vertical-datums/local-mean-sea-level-datums), essentially the same as during the Irwin (1982) survey which reported the lake level at 339.465 m above mean sea level for the same datum. For practical purposes, the lake level has been considered static during our survey (i.e., <5 mm variation).

The MBES was patch tested prior to the survey; however, it was possible to refine the roll and pitch bias values when sounding the deep, flat section of the lake. Data was post-processed with the updated values to obtain fully corrected bathymetry. Sound velocity in the area was found to be relatively consistent at around 1485m/s until a noticeable thermocline at around 16 m depth, thereafter decreasing to about 1468m/s close to 30 m depth (cf. Walker et al., this issue). Sound velocity observations were conducted daily to ensure MBES data was refraction corrected during post processing.

MBES survey lines were run to ensure at least 50% overlap with adjacent lines; that is, successive lines were run just inside the edge of the previous MBES coverage to achieve high data density and provide a level of navigation safety. No set line spacing was run due to the variable depths and changing swath width. Full MBES coverage was achieved from around the 5 m contour to the maximum depth of the lake. Vessel speed was generally kept to between 4 and 5 knots.

A basic assessment of depth accuracy has been made based on the various component sources of error likely to be experienced during the survey (e.g., vessel draught setting, EM3002D instrument accuracy, heave uncertainty) which equated to 16 cm in 5 m water depth, 31 cm in 50 m and 54 cm in 100 m. Data quality checks and post processing of survey data was carried out in Caris HIPS (v. 7.1). A significant amount of noise was present in depth data due to gas present in the water column; this was clearly evident during sounding operations where numerous gas plumes were observed (see below). The majority of this noise was easily identifiable and removed using a combination of manual and automated filters.

Lakefloor photography

Deep-sea digital cameras from the Woods Hole Oceanographic Institution were configured into small, hand-deployed packages that could be used from the University of Waikato vessel *Taitimu*. The 2011 system included a DeepSea Power and Light (DSPL) 3.3 megapixel camera (based on a Nikon 995 digital 'point-and-shoot' camera), and the 2014 system consisted of an Ocean Imaging Systems (OIS) 16 megapixel camera, a 6000 m-rated color digital camera that utilizes a Nikon D7000 single-lens reflex camera as the imaging module with a 20 mm lens behind a water-corrected dome. The cameras were coupled to a 150 Watt/sect strobe in a 1000 m-

rated Delrin housing to provide illumination and NiMH battery packs to provide power for all the sensors. A depth sensor (SeaBird Instruments SBE-50) and an altimeter (Valeport 500 KHz) were also used to determine both depth and altitude, respectively, above the lake bottom at a 1 Hz rate. The aluminum and syntactic foam frame that enclosed all the components in the 2014 system was approximately 0.75 m diameter and weighed ~40 kg in air and 20 kg in water. Images in 2011 were acquired every ~10 sec using an exposure of F2.8 and shutter speed of 1/60 sec and an ISO of 400; images in 2014 were acquired every 8 sec using an exposure of F3.5 and shutter speed of 1/60 sec, and an ISO of 400. All images were processed using Adobe Photoshop™ standard correction algorithms for tone, contrast and color and variable shadow/highlight adjustment depending on the subject matter. Because of variable water clarity near the lake bottom, images were acquired from altitudes that usually ranged between 1 and 3 m. In general, the scale across the photos maps to the altitude of the camera directly, for both cameras.

Seismic surveys

Seismic reflection surveying of Lake Rotomahana was largely done using a Boomer system comprising an 8-channel, 1.5625m group interval GEOEEL streamer sampled at 8KHz and a CSP 300 power source coupled to a *HyroAcoustics* AA200 boomer plate. In addition, an *Edgetech* 216 CHIRP system was used in select surveys. Wide-area DGPS navigation was recorded by a *Hydropro* navigation system while aboard the *Taitimu*.

The Rotomahana Boomer seismic lines were processed with a standard processing sequence using the GLOBE Claritas™ seismic processing software. The raw shot data were read, missing traces were inserted, and FK (Fourier K, or wave number)

mute was used to remove both low and high frequency noise in the FK domain. An auto-mute was used to automatically mute noisy traces, a convolution filter for minimum phase conversion, deconvolution applied, then sorting from shots to common depth point also known as common midpoint (CDP/CMP).

The lake bottom was digitized using a guided picking function. Normal moveout was applied using a 1D trend following the lake bottom. The short offset of the streamer made it impossible to obtain meaningful stacking velocities, so a simple 1D trend was used using 1500 m/s for water velocity and 2500 m/s for the velocity at 500 ms below the lake bottom. Interactive velocity analysis showed the CDP data to be insensitive to changes in velocity due to the very short offset between shot and receiver of 25 m.

All data were muted 15 ms above the digitised lake bottom. The data were then stacked, and non-live traces removed. Finite difference migration was applied using the same 1D trend as before. The migrated seismic data amplitudes were linearly scaled using time/scale values of 0 ms/1 and 100 ms/10 below the lake bottom. An FK filter was used to remove frequencies above 2000 Hz. A spectral whitening function was applied to increase the weighting of frequencies at 1200 Hz (2.0) and 1500 Hz (1.5) relative 100 Hz (0.5). Shot coordinates were added to the trace headers, textual headers were populated with survey metadata, and output files were written in standard SEGY format.

In contrast to the boomer data, the CHIRP (compressed high intensity radar pulse) did not perform well on the steeply dipping parts of the lake. The chirp data are highly diffractive on these slopes, and it is difficult to interpret any structure from either the correlate or the envelope. Despite various different processing approaches including several coherency filters and post-stack time migration, no improvement

was achieved. However, flat lying sediments in the lake were imaged noticeably better (e.g., there is a good correspondence between the flat lying sediments of CHIRP Line 100 with boomer Line L00; see Fig. 9B) and shows small scale features that the boomer is not able to resolve. However, the gassy water column and sediments hindered the CHIRP signals from penetrating very deeply.

Processing of the CHIRP data was much simpler because it uses a single channel with no source-receiver offset. Input files were converted from a proprietary format to standard SEGY. Shot coordinates were incorrect in the file headers, so were replaced with values recorded from the GPS system. Digitised lake-bottom times were added to the trace headers, and the data were scaled using time/scale pairs of 0 ms/1 and 50 ms/30 below the lake bottom.

Bubble plume survey

A *Lowrance* HDS8 sounder with a 200 KHz transducer was used to detect the bubble plumes following a pre-survey plan using Garmin MapSource employing 30 m line spacing. The plan was then loaded into both a Garmin GPS MAP 60cx and a Garmin GPS MAP78s for redundancy. Each time the GNS Science boat drove over a plume a waypoint was created and its number and the type of plume encountered was logged. Bubble plumes recorded by the sounder were divided into five categories based on the acoustic appearance of the plumes, ranging from; 1) diffuse, where single plumes were just detectable rising from the lakefloor, 2) weak, where single plumes rose to the thermocline, 3) moderate, where multiple plumes rose to, and locally just breached, the thermocline, 4) strong, where large single plumes clearly breached the thermocline and reached the lake surface, and 5) very strong, where multiple plumes clearly breached the thermocline and reached the surface (Fig. 15).

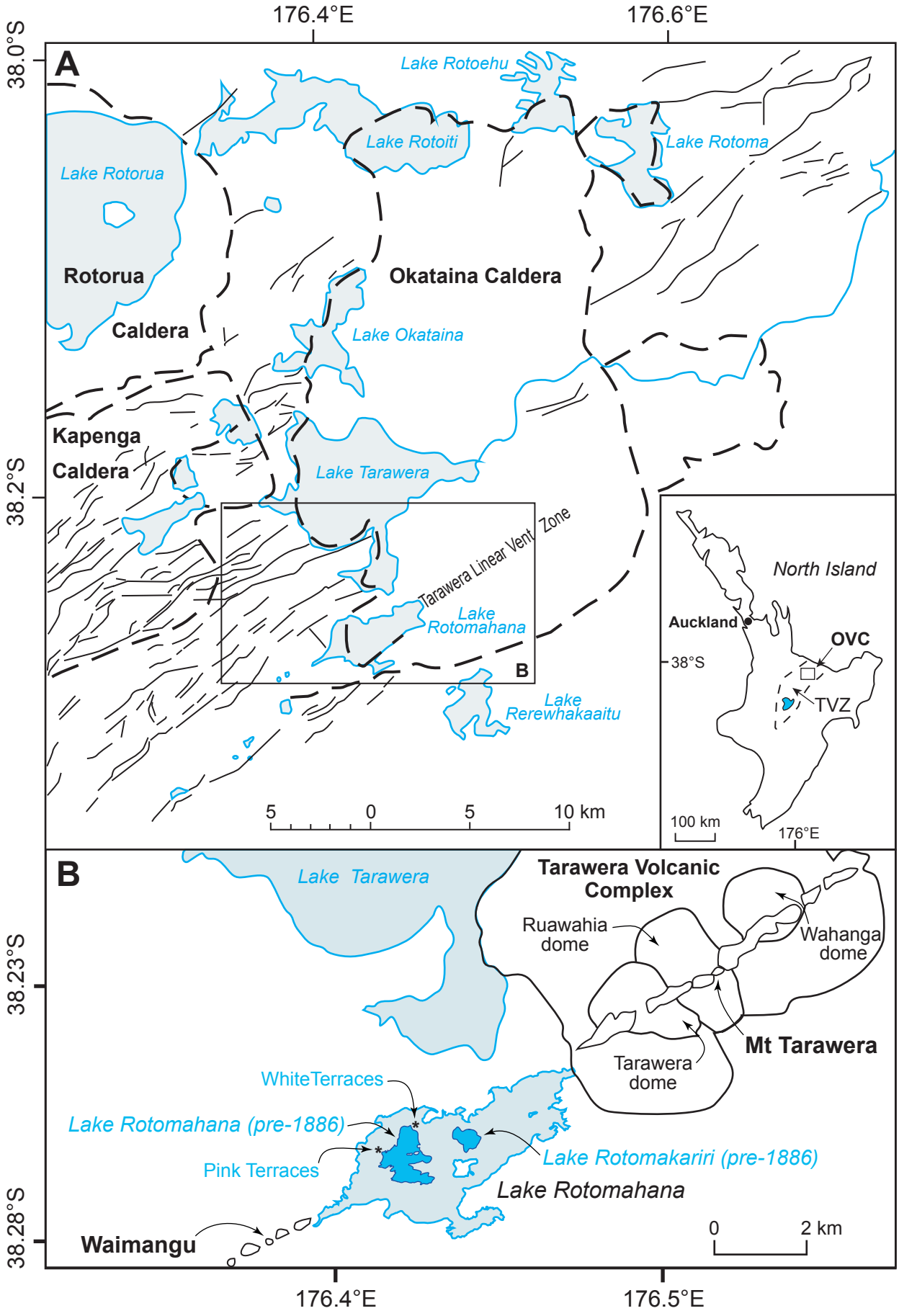
176.4°E
176.6°E
38.0°S
38.2°S
A
Lake Rotoehu
Lake Rotoiti
Lake Rotoma
Lake Rotorua
Rotorua
Caldera
Okataina Caldera
Lake Okataina
Kapenga
Caldera
Lake Tarawera
Tarawera Linear Vent Zone
Lake
Rotomahana
B
Lake
Rerewhakaaitu
5
0
5
10 km
North Island
Auckland
OVC
38°S
TVZ
100 km
176°E
B
38.23°S
38.28°S
Lake Tarawera
Tarawera Volcanic
Complex
Ruawahia
dome
Wahanga
dome
Mt Tarawera
Tarawera
dome
WhiteTerraces
Lake Rotomahana (pre-1886)
Pink Terraces
Lake Rotomakariri (pre-1886)
Lake Rotomahana
Waimangu
0
2 km
176.4°E
176.5°E

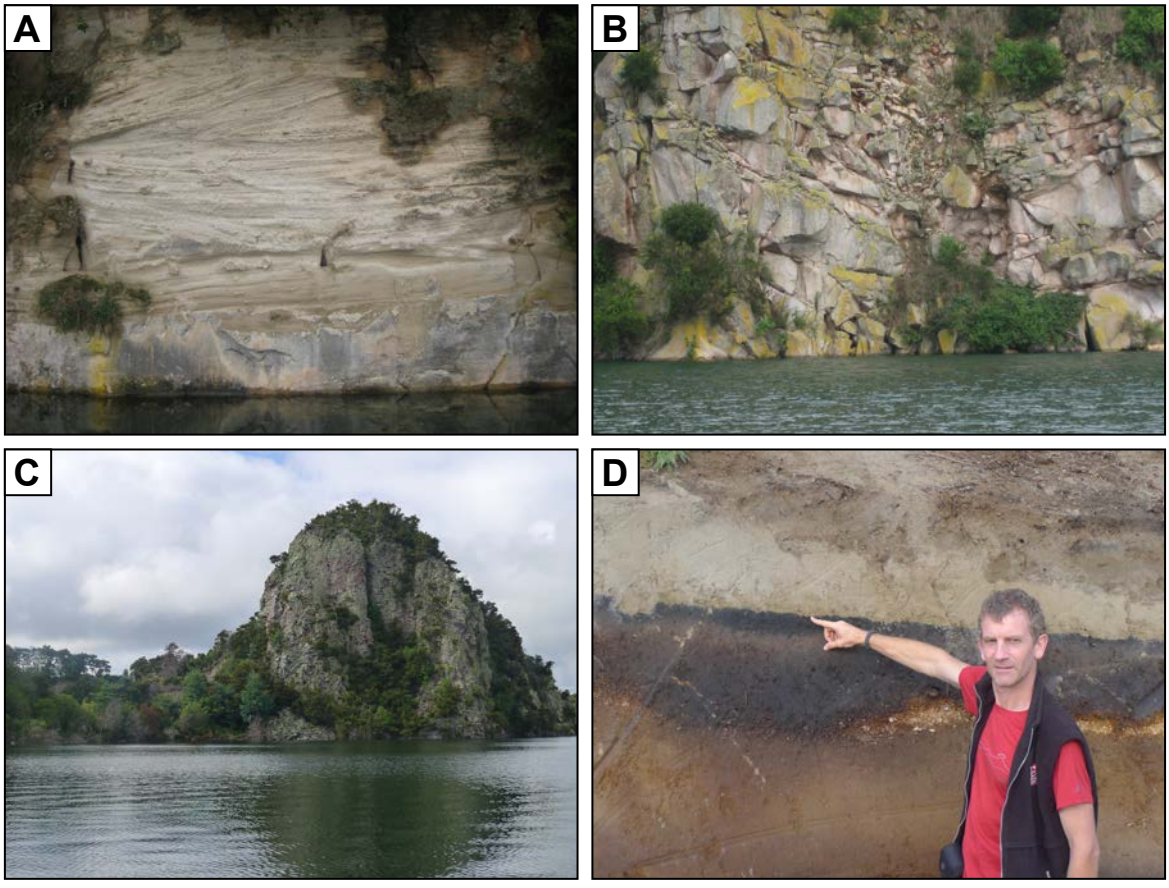
A
B
C
D

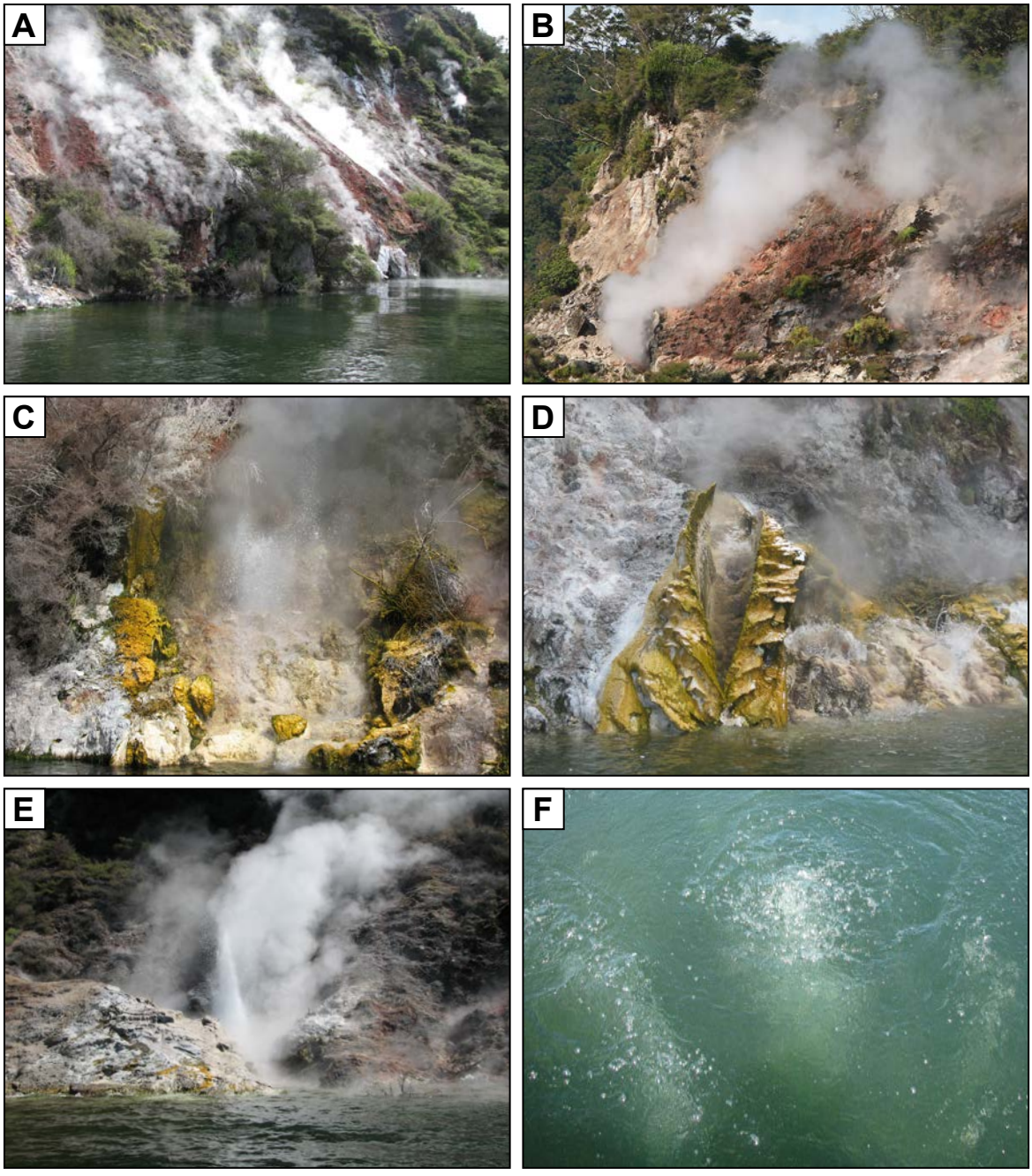
A
B
C
D
E
F

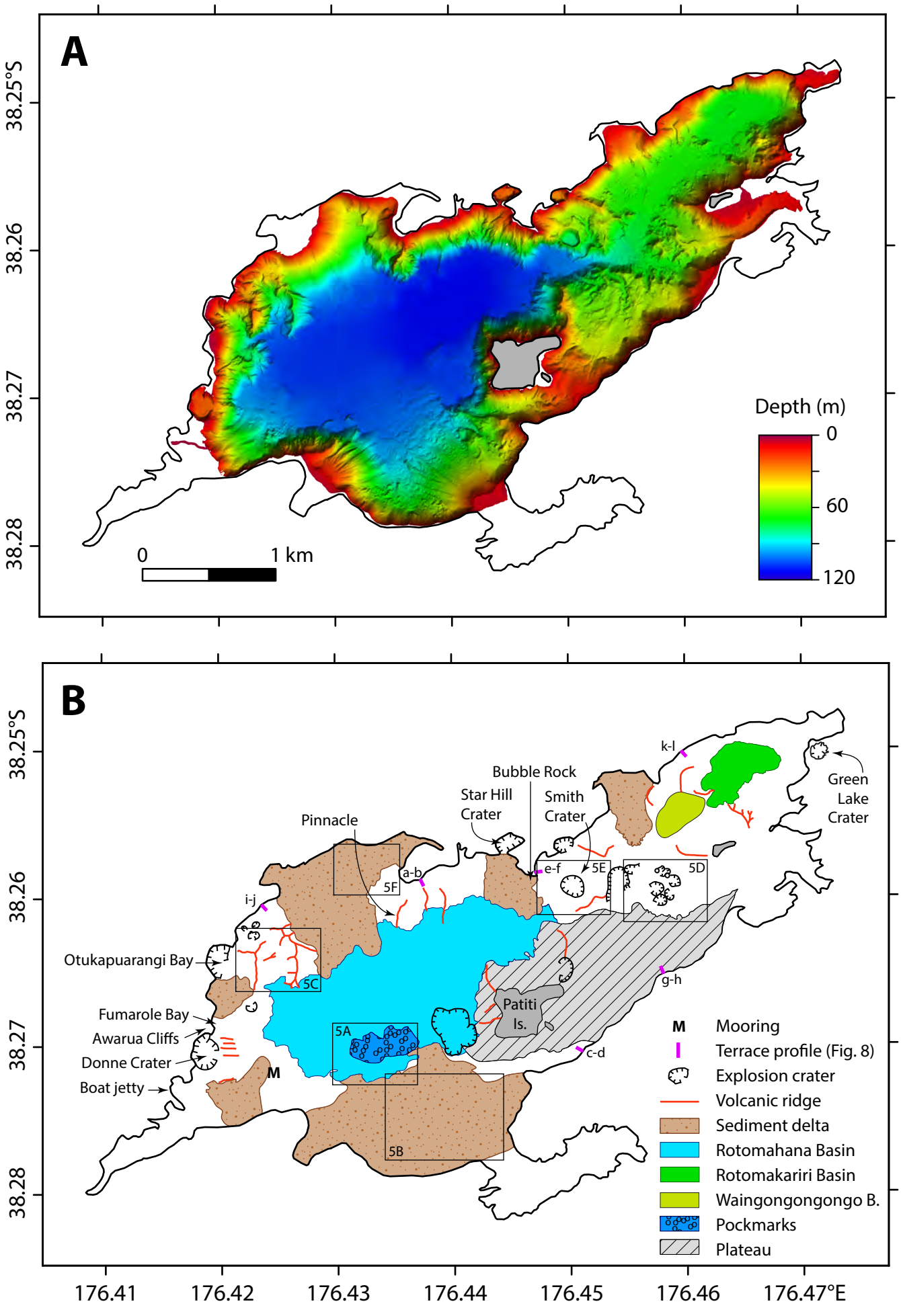
A
38.25°S
38.26
38.27
38.28
0
1 km
Depth (m)
0
60
120
B
38.25°S
38.26
38.27
38.28
176.41
176.42
176.43
176.44
176.45
176.46
176.47°E
Bubble Rock
Star Hill Crater
Smith Crater
Pinnacle
k-l
Green Lake Crater
a-b
e-f
5E
5D
5F
i-j
Otukapuarangi Bay
5C
g-h
Fumarole Bay
Awarua Cliffs
Donne Crater
Boat jetty
M
5A
Patiti Is.
c-d
5B
M Mooring
Terrace profile (Fig. 8)
Explosion crater
Volcanic ridge
Sediment delta
Rotomahana Basin
Rotomakariri Basin
Waingongongongo B.
Pockmarks
Plateau

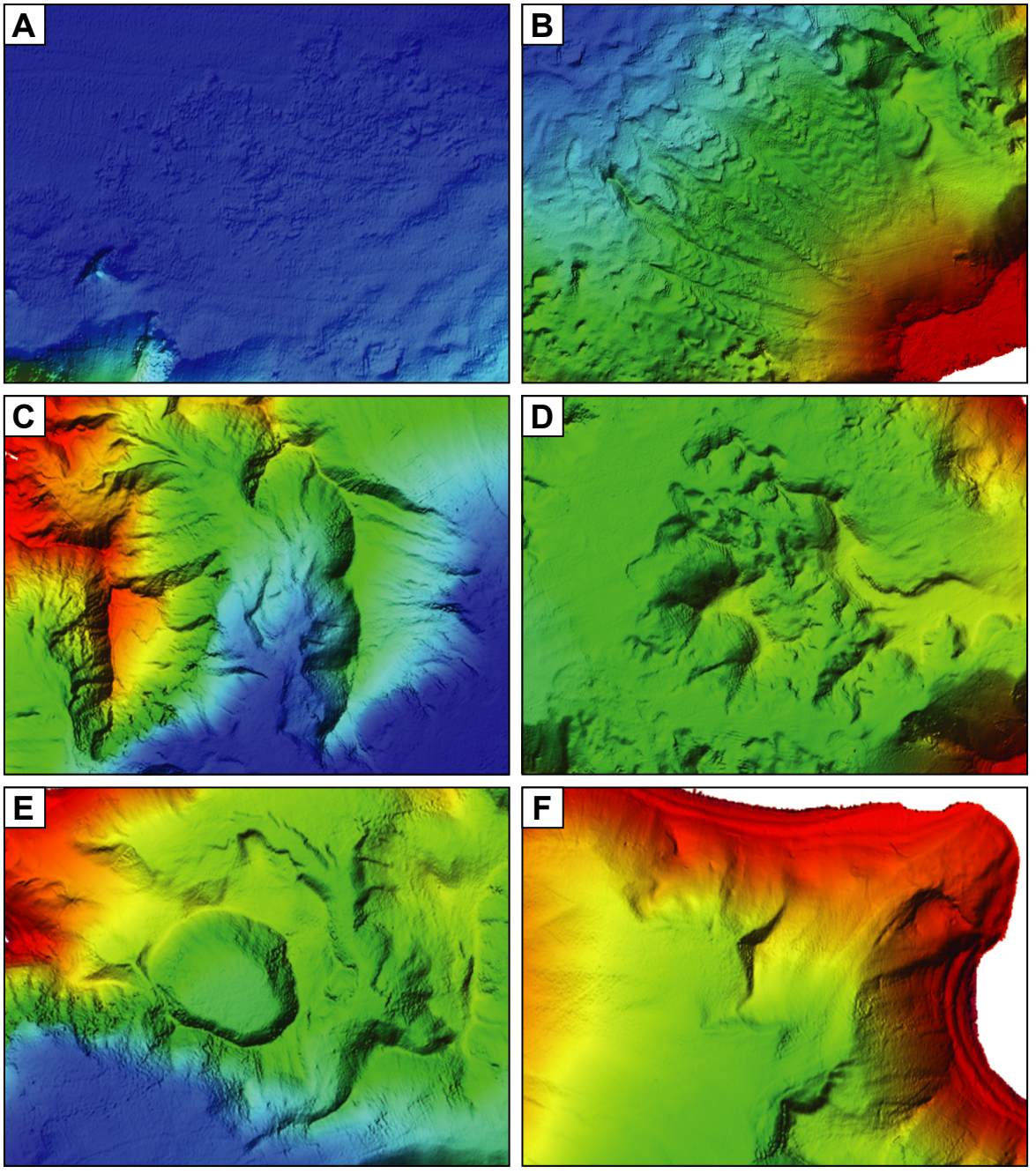
A
B
C
D
E
F

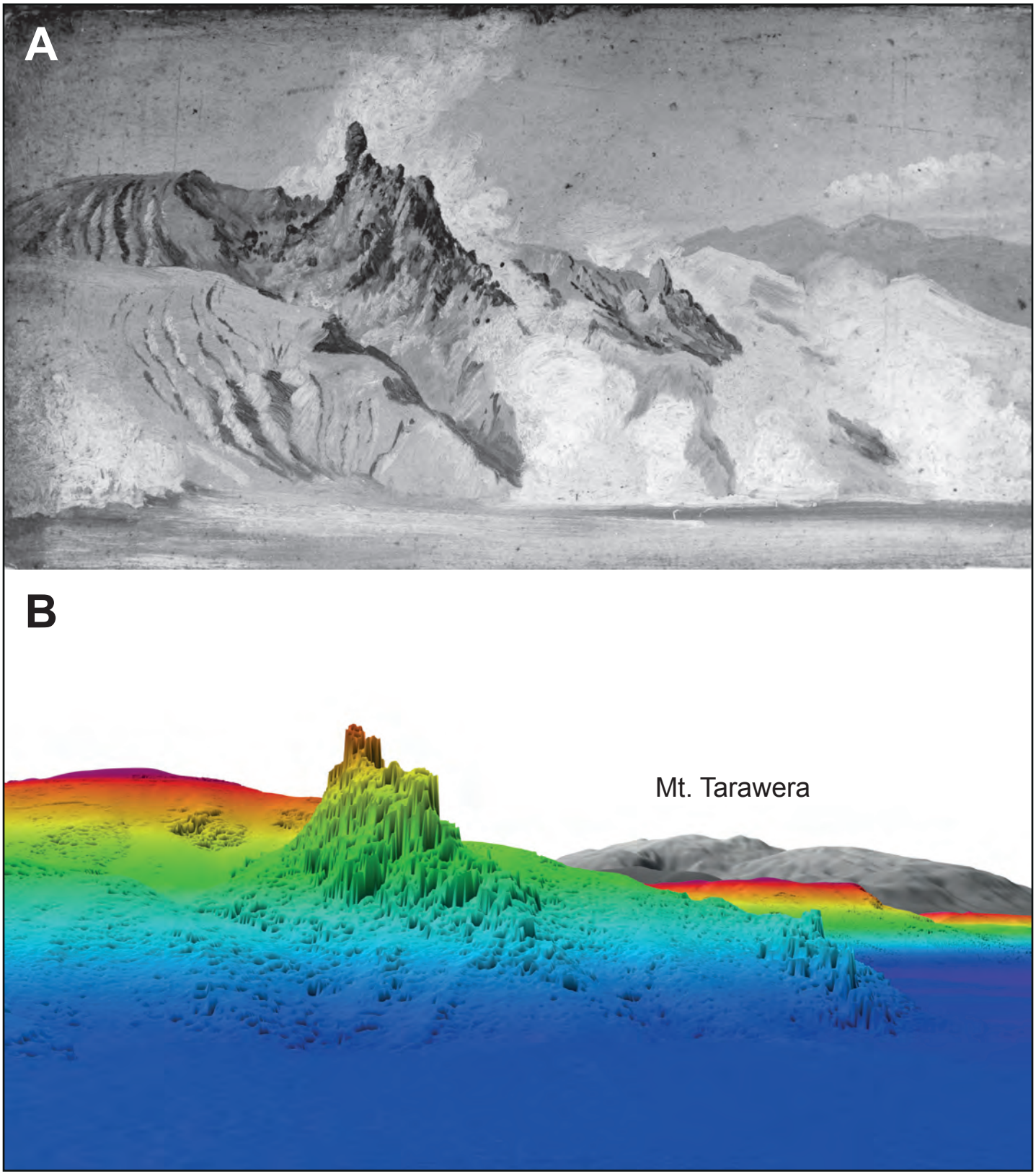
A
B
Mt. Tarawera

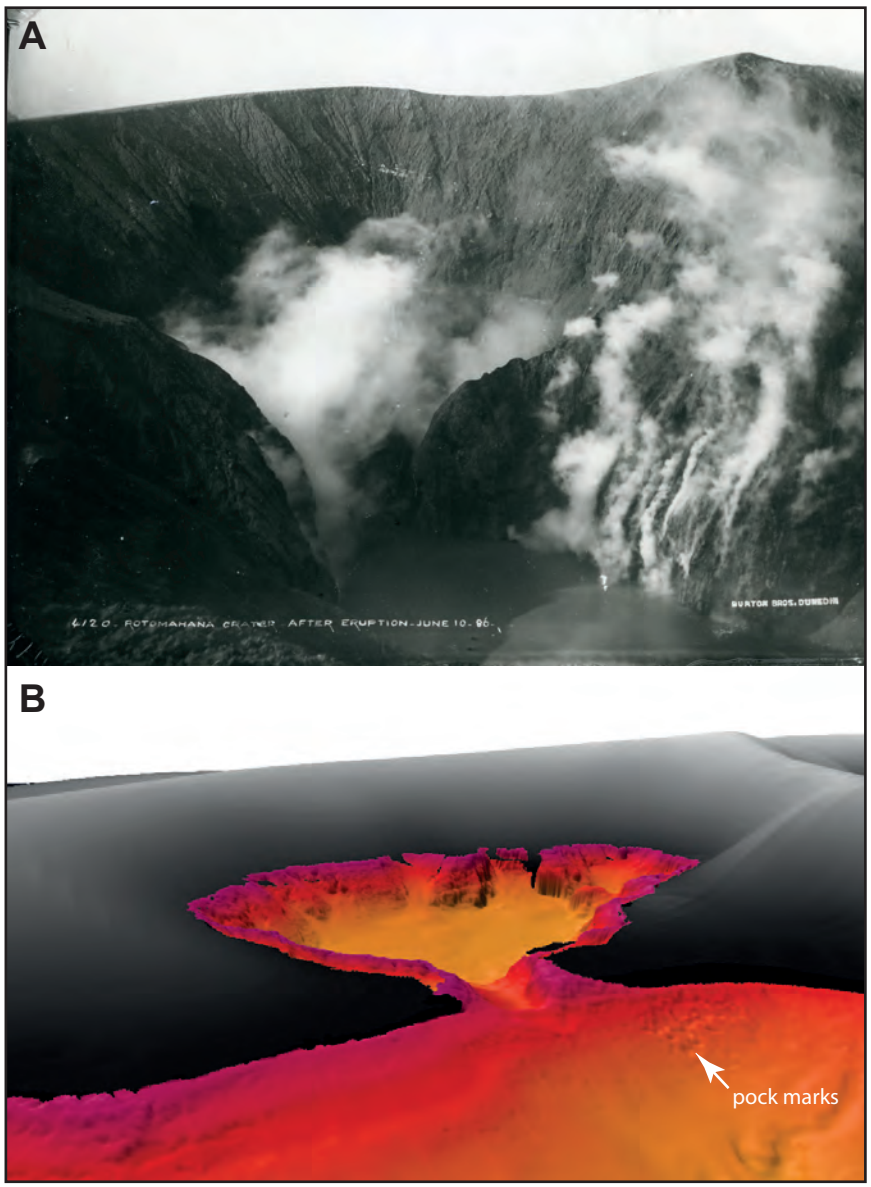
A
6/12.0. ROTOMAHANA CRATER AFTER ERUPTION. JUNE 10. 86.
BURTON BROS. DUNEDIN
B
pock marks

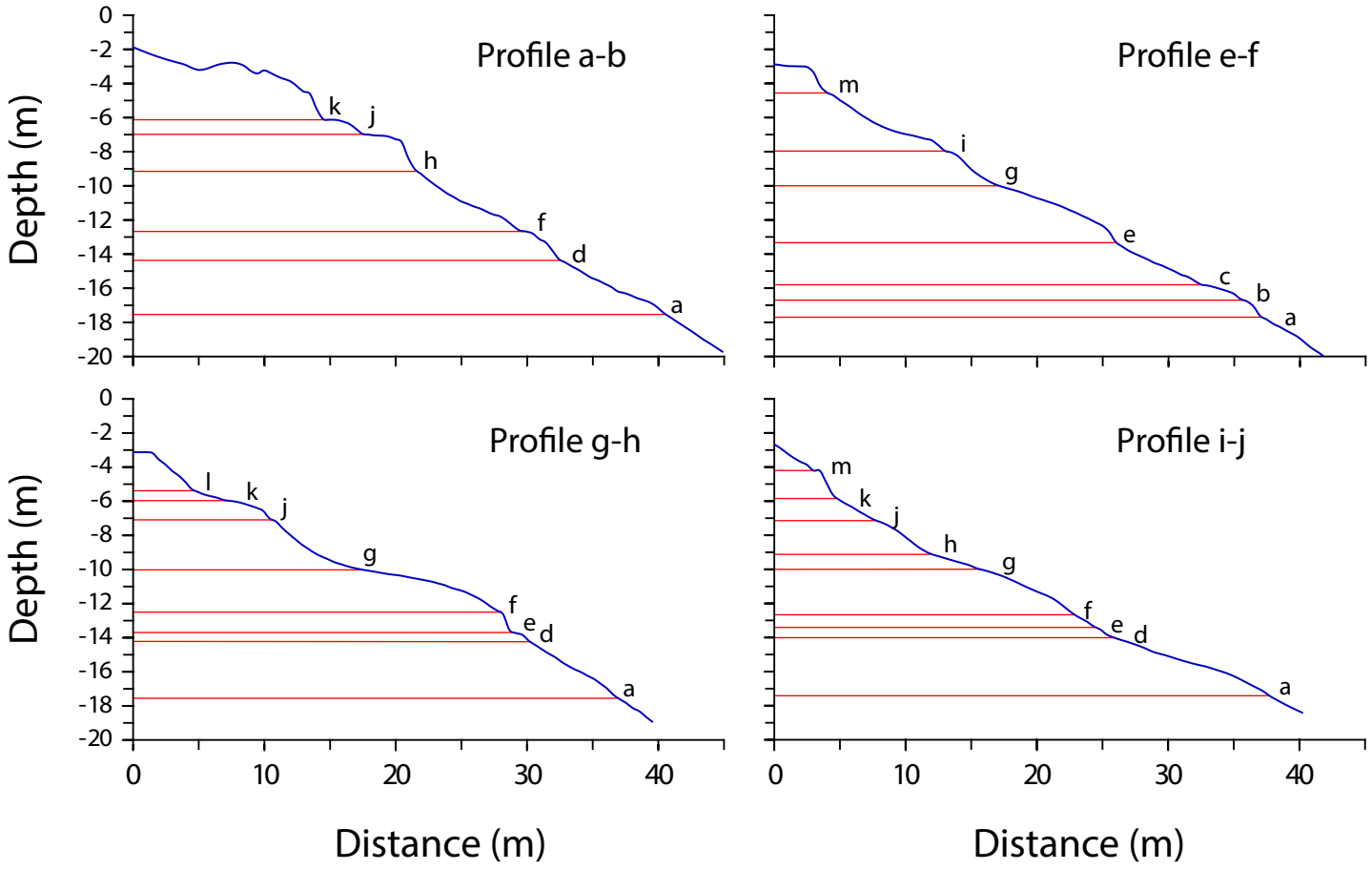
Profile a-b
Profile e-f
Profile g-h
Profile i-j
Depth (m)
Depth (m)
Distance (m)
Distance (m)
0
-2
-4
-6
-8
-10
-12
-14
-16
-18
-20
0
10
20
30
40
a
b
c
d
e
f
g
h
i
j
k
l
m

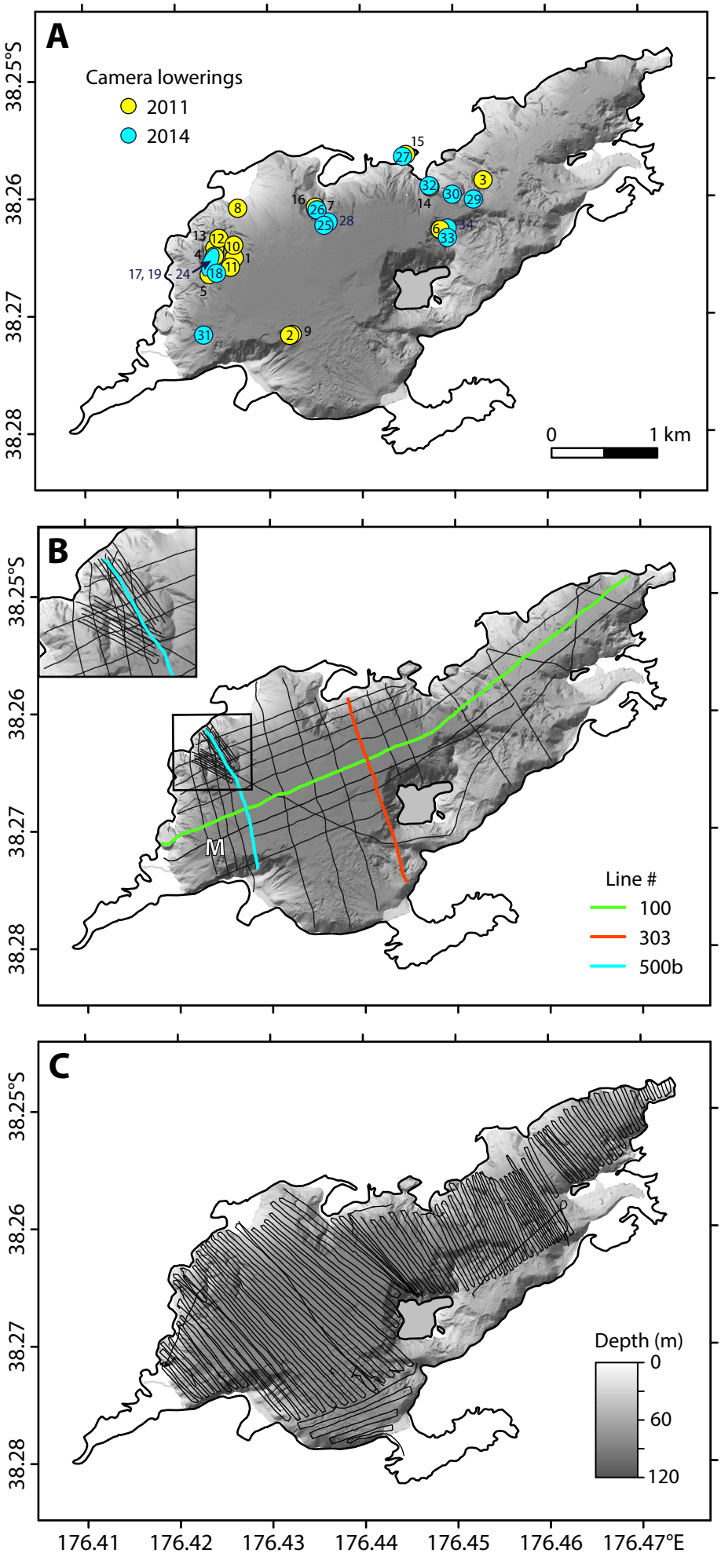
A
Camera lowerings
2011
2014
38.25°S
38.26
38.27
38.28
0
1 km
B
M
Line #
100
303
500b
C
Depth (m)
0
60
120
176.41
176.42
176.43
176.44
176.45
176.46
176.47°E

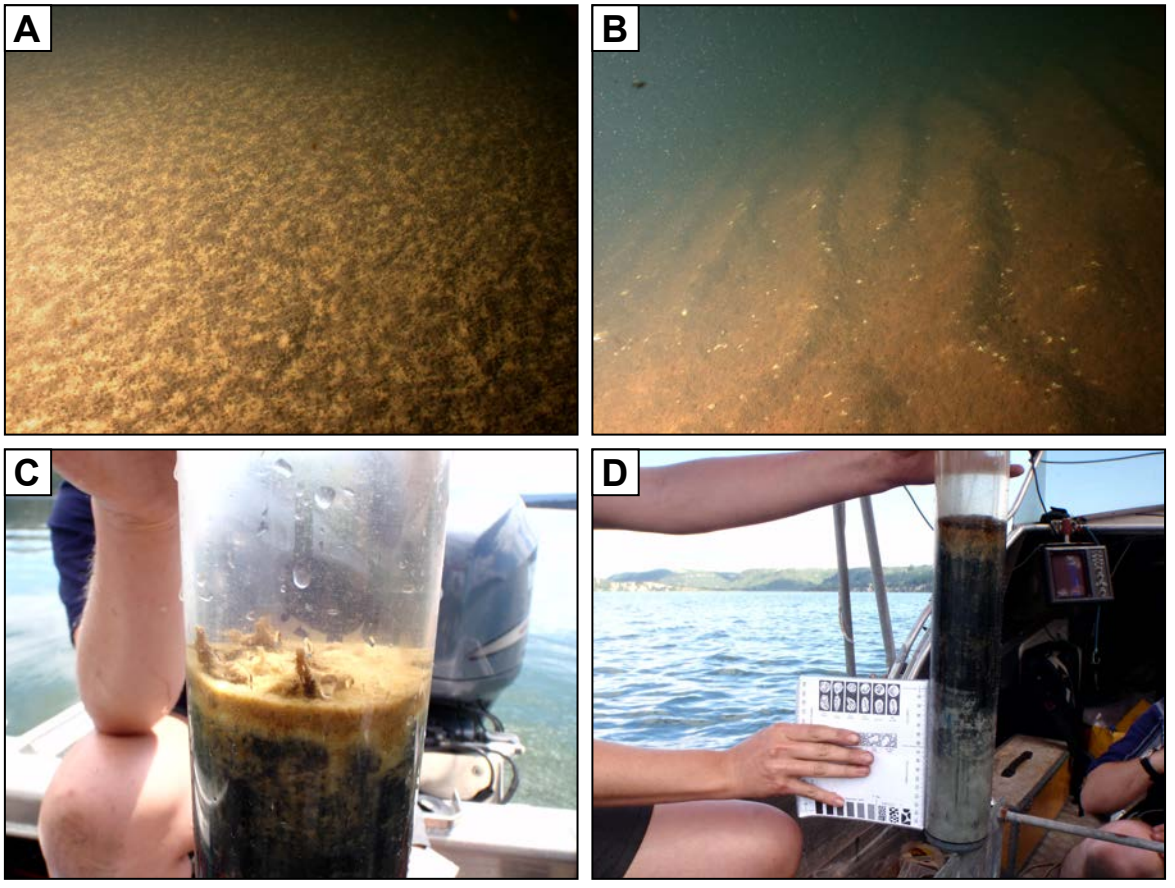
A
B
C
D

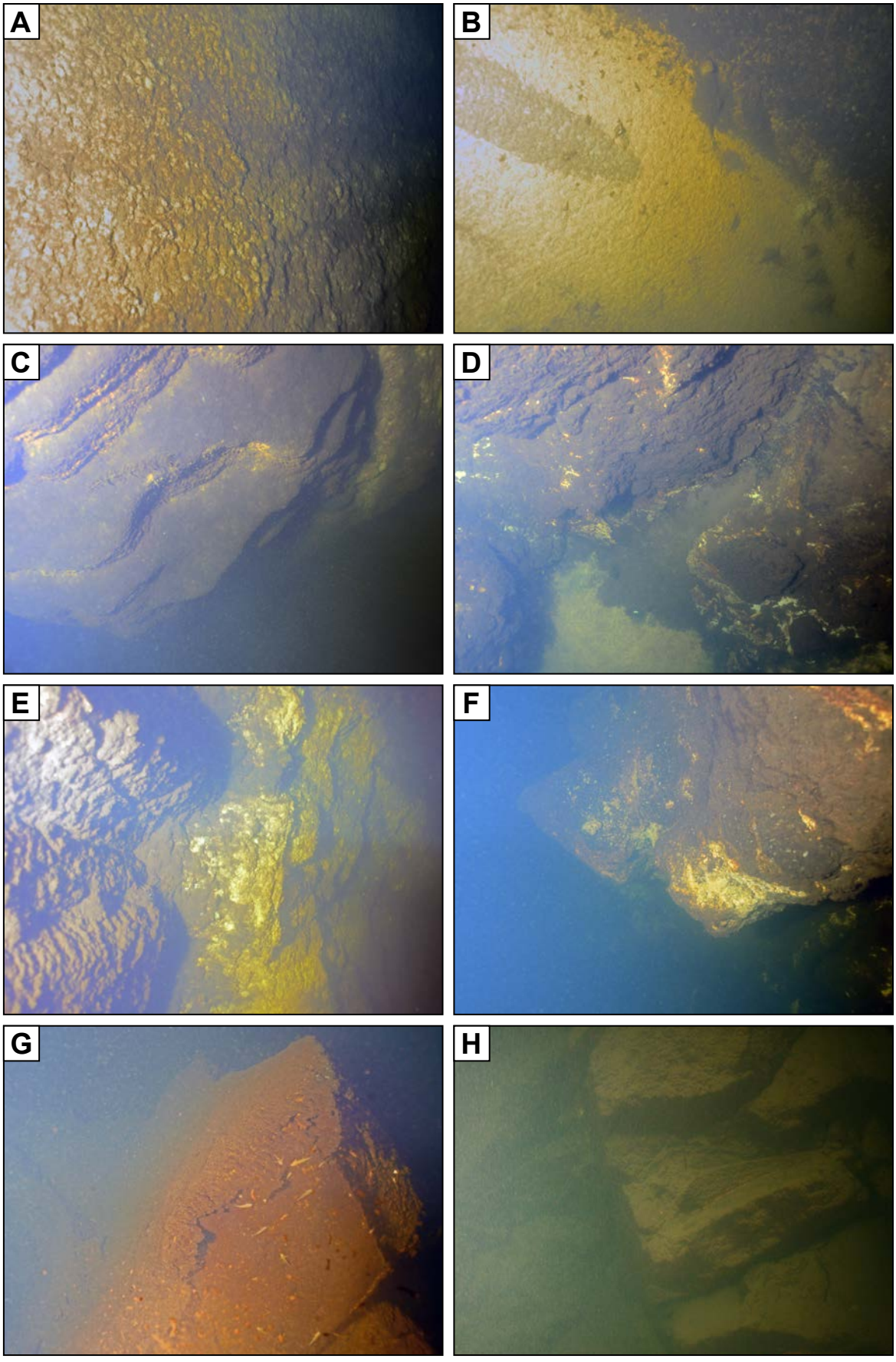
A
B
C
D
E
F
G
H

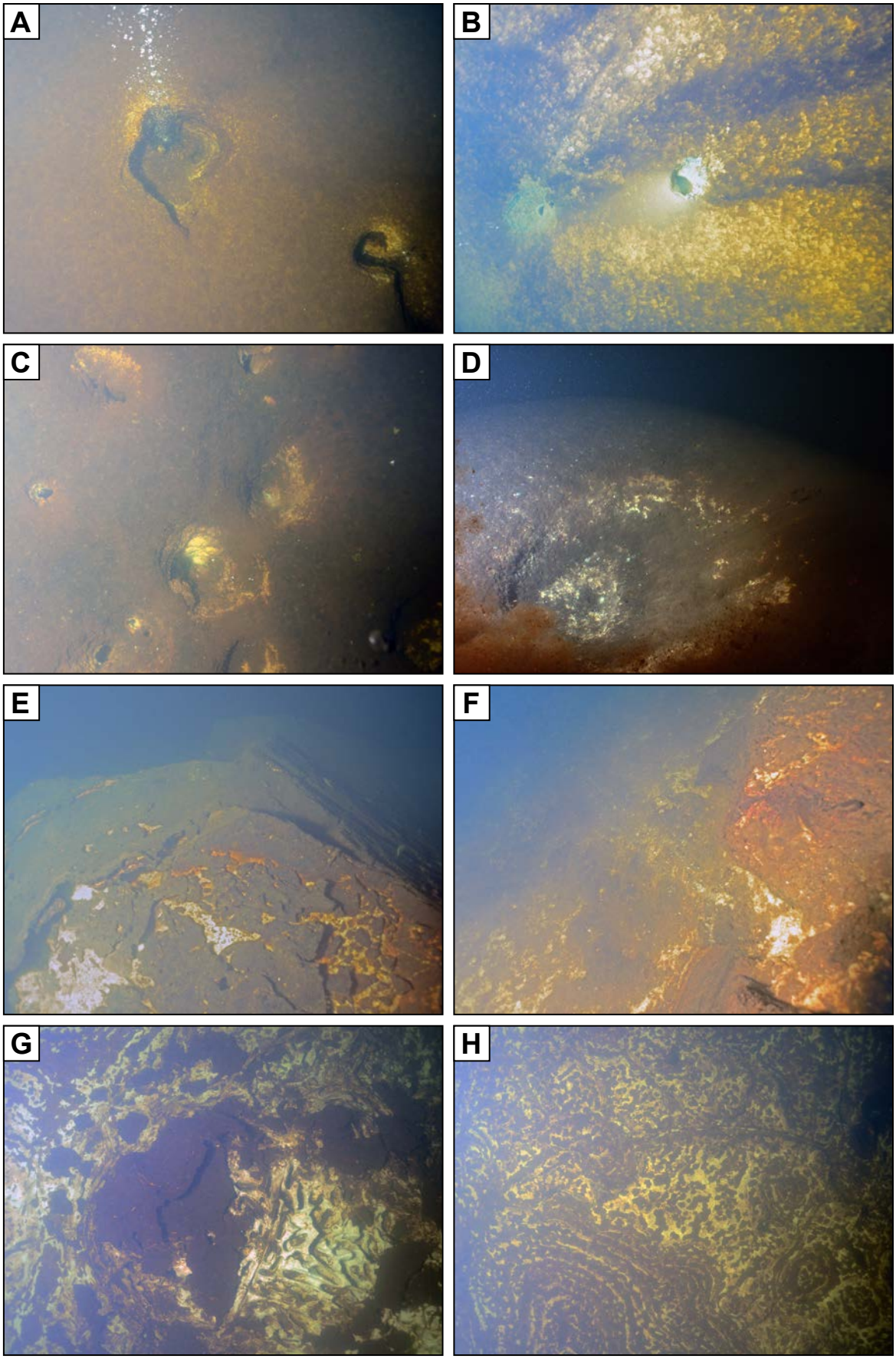
A
B
C
D
E
F
G
H

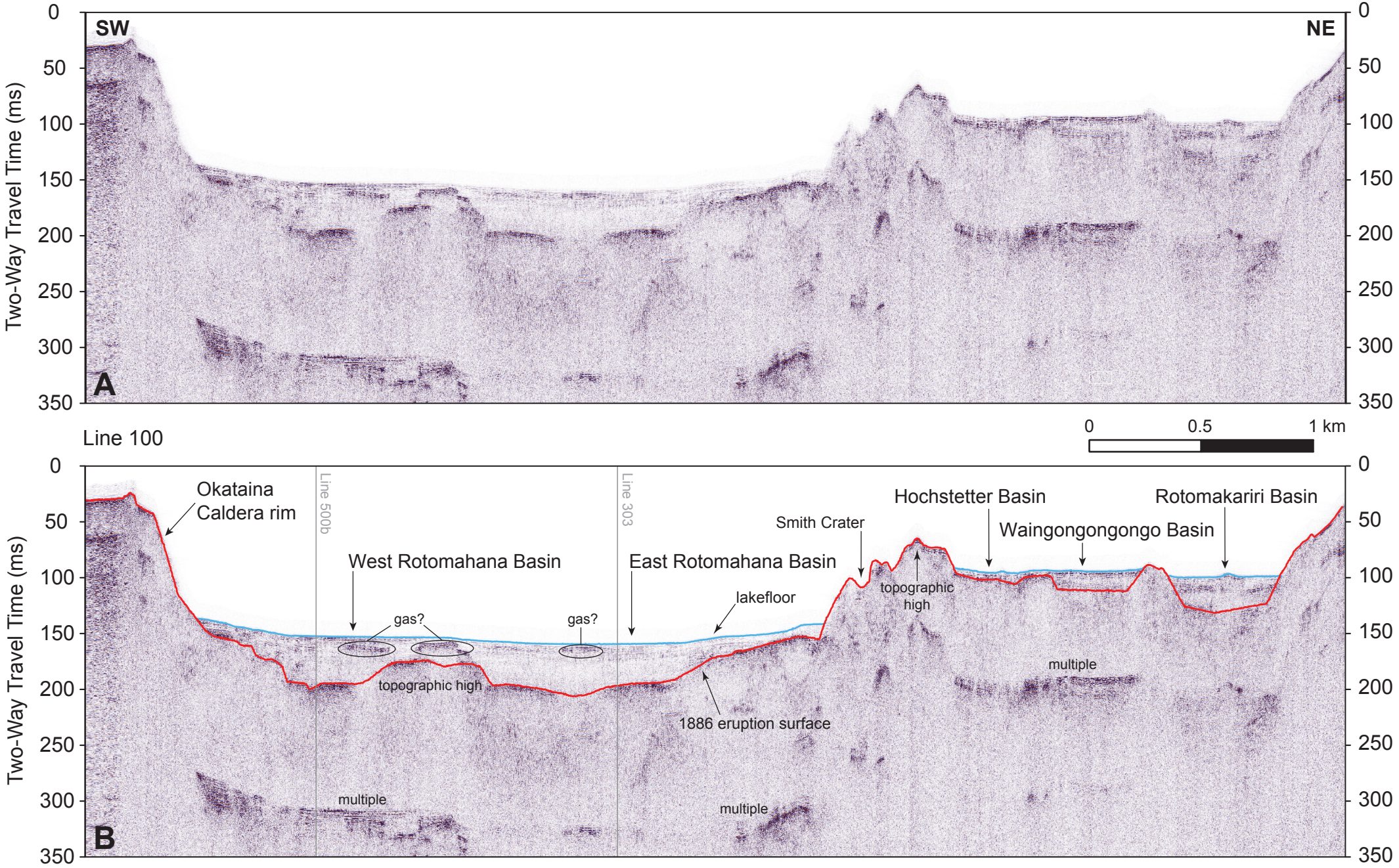
SW
NE
A
Two-Way Travel Time (ms)
0
50
100
150
200
250
300
350
Line 100
0
0.5
1 km
B
Okataina
Caldera rim
Line 500b
Line 303
West Rotomahana Basin
East Rotomahana Basin
Smith Crater
Hochstetter Basin
Waingongongongo Basin
Rotomakariri Basin
lakefloor
topographic
high
gas?
gas?
topographic high
1886 eruption surface
multiple
multiple
multiple

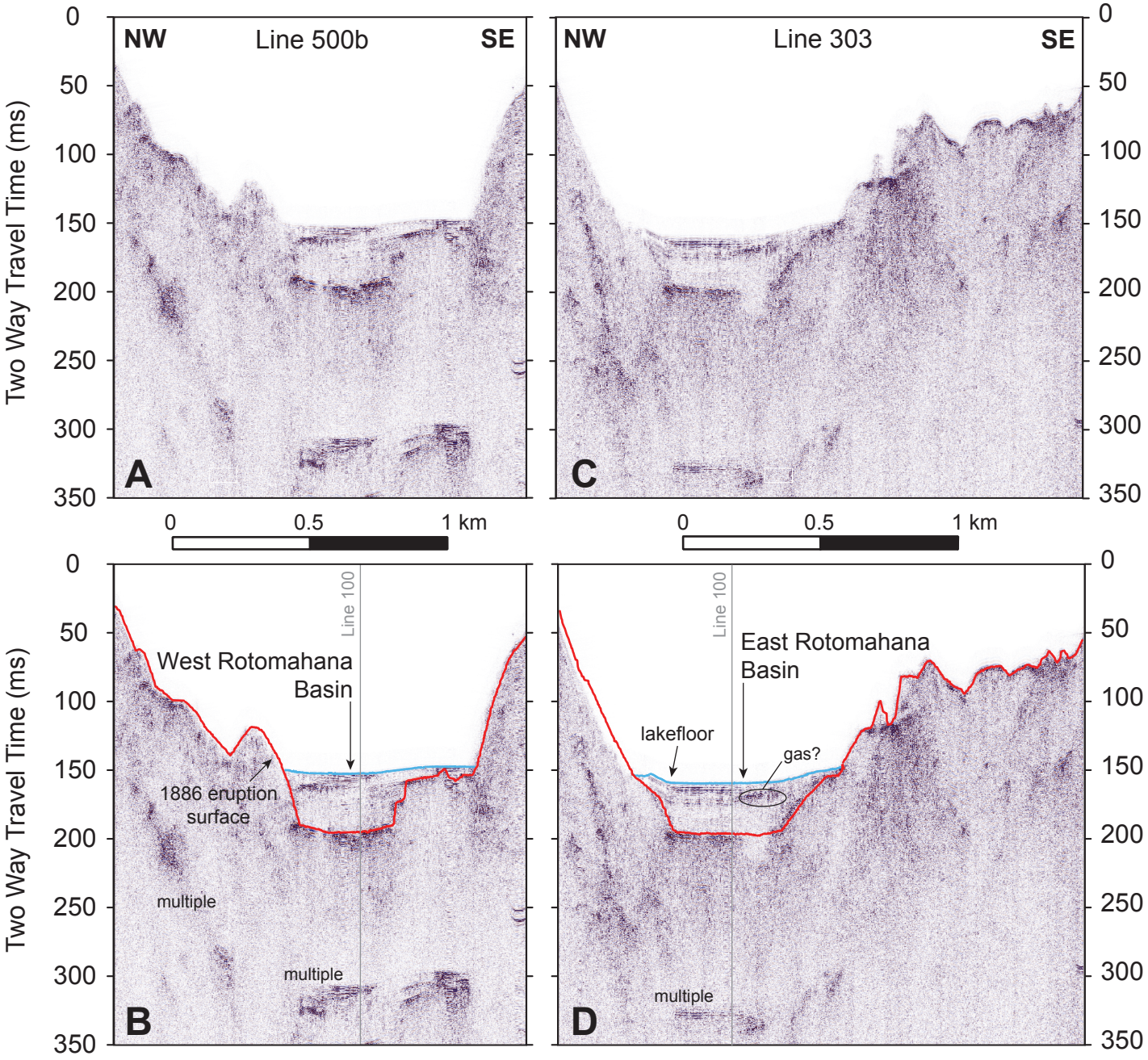
Two Way Travel Time (ms)
0
50
100
150
200
250
300
350
NW
Line 500b
SE
A
0
0.5
1 km
NW
Line 303
SE
C
Line 100
West Rotomahana Basin
1886 eruption surface
multiple
multiple
B
Line 100
East Rotomahana Basin
lakefloor
gas?
multiple
D

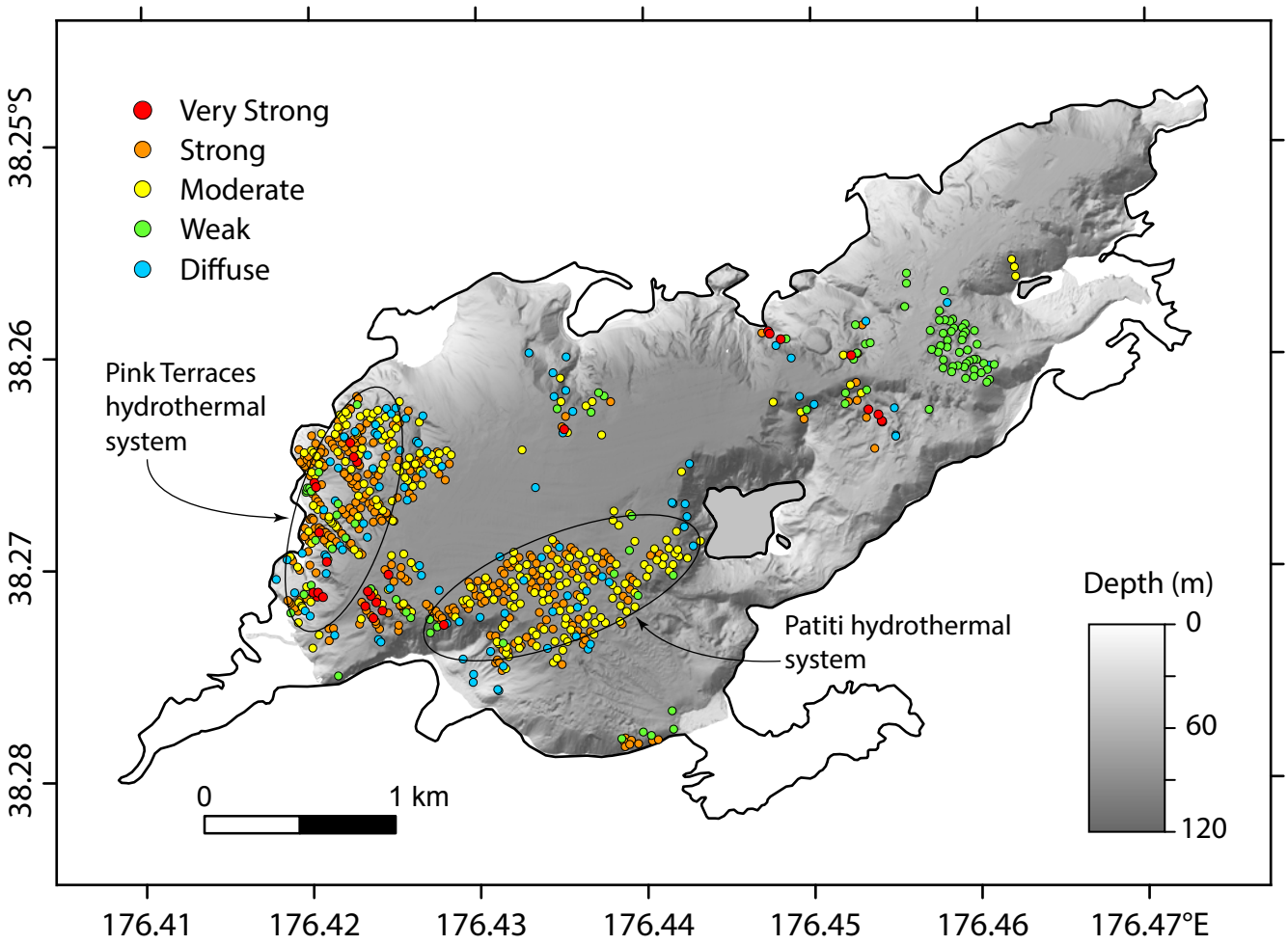
Very Strong
Strong
Moderate
Weak
Diffuse
Pink Terraces
hydrothermal
system
Patiti hydrothermal
system
Depth (m)
0
60
120
0
1 km
38.25°S
38.26
38.27
38.28
176.41
176.42
176.43
176.44
176.45
176.46
176.47°E

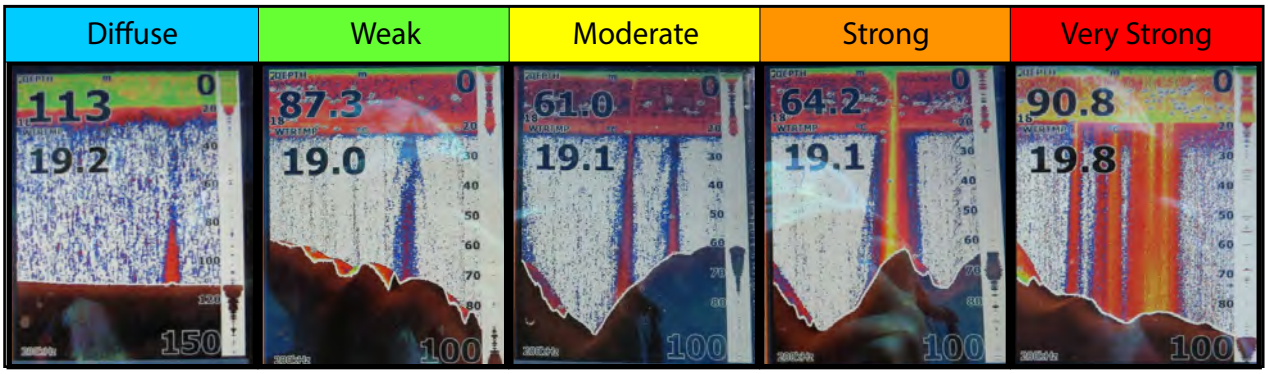
Diffuse
Weak
Moderate
Strong
Very Strong
113
19.2
87.3
19.0
61.0
19.1
64.2
19.1
90.8
19.8

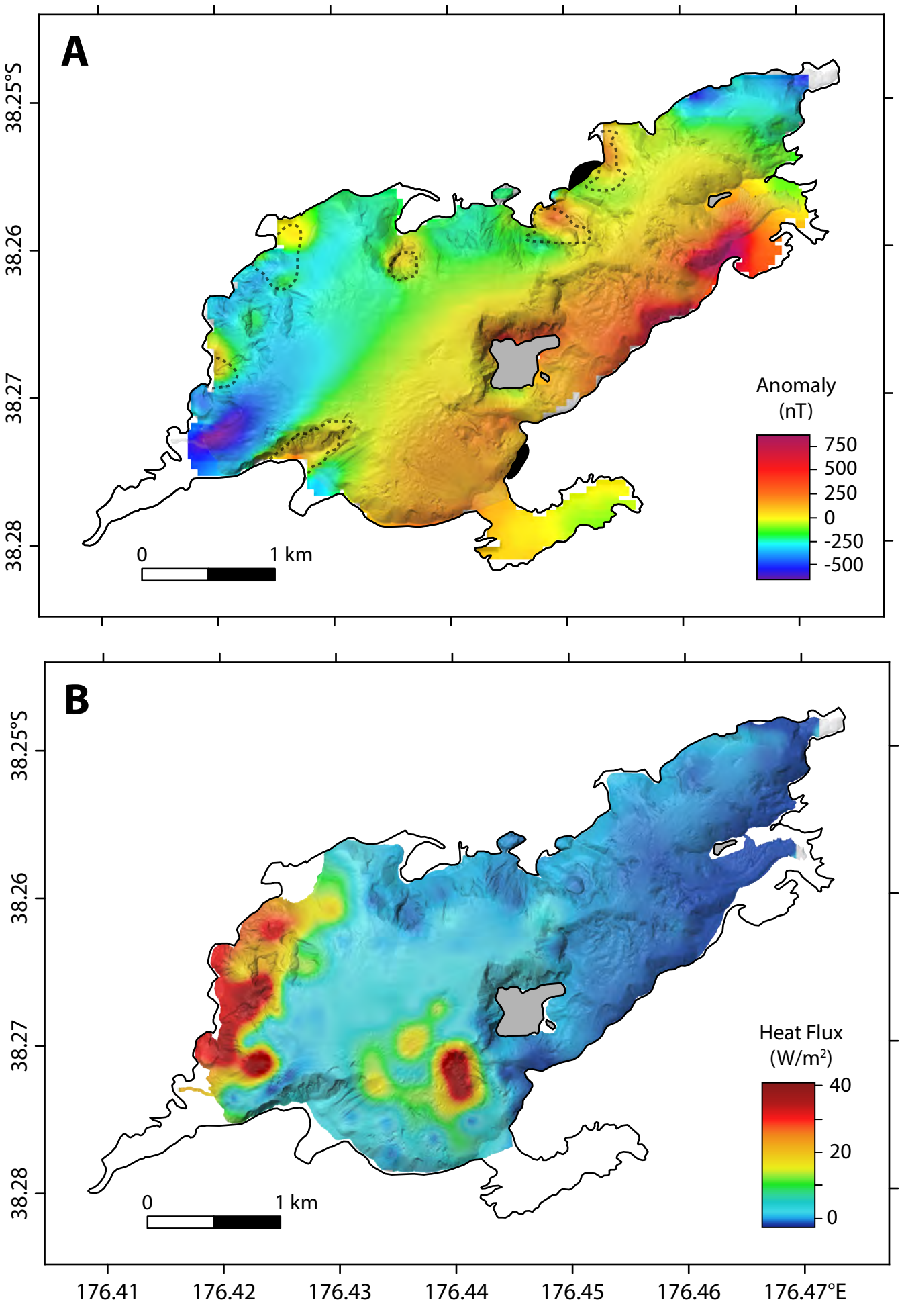
A
38.25°S
38.26
38.27
38.28
0
1 km
Anomaly
(nT)
750
500
250
0
-250
-500
B
38.25°S
38.26
38.27
38.28
0
1 km
Heat Flux
(W/m²)
40
20
0
176.41
176.42
176.43
176.44
176.45
176.46
176.47°E

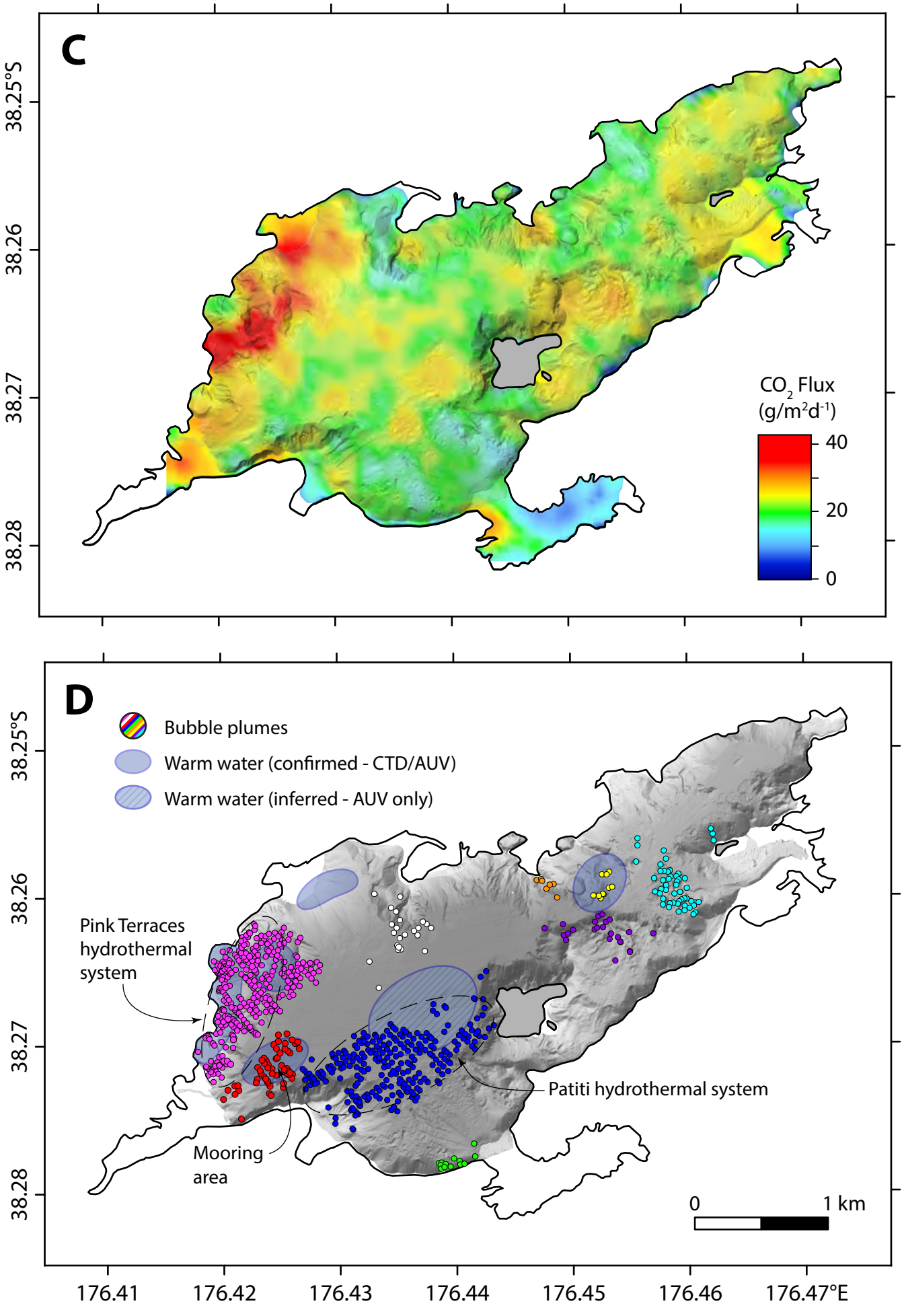
C
38.25°S
38.26
38.27
38.28
CO2 Flux
(g/m2d-1)
40
20
0
D
Bubble plumes
Warm water (confirmed - CTD/AUV)
Warm water (inferred - AUV only)
Pink Terraces
hydrothermal
system
Patiti hydrothermal system
Mooring
area
0
1 km
176.41
176.42
176.43
176.44
176.45
176.46
176.47°E

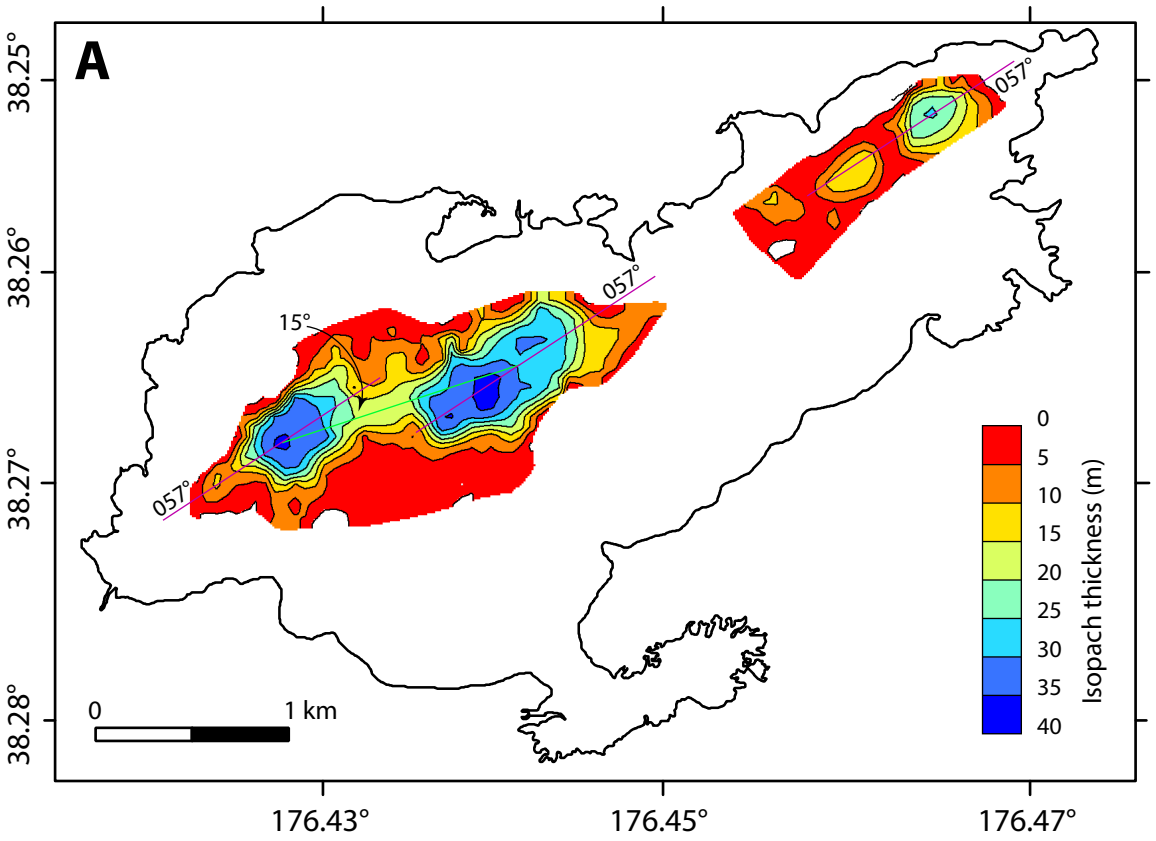
A
38.25°
38.26°
38.27°
38.28°
176.43°
176.45°
176.47°
057°
15°
057°
057°
0
1 km
Isopach thickness (m)
0
5
10
15
20
25
30
35
40

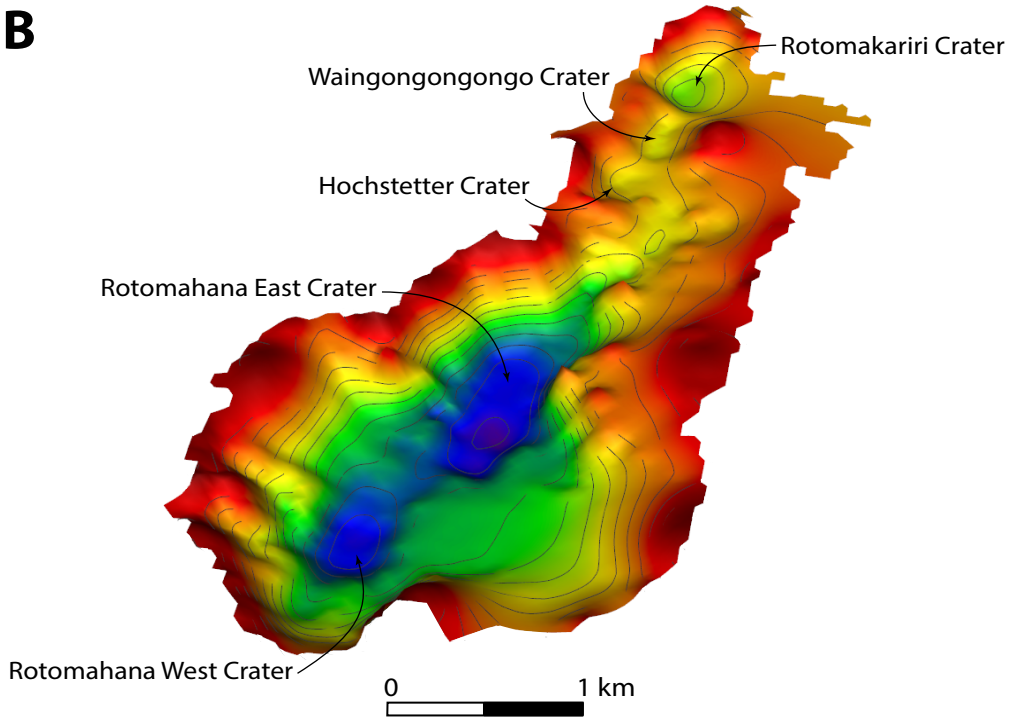
B
Rotomakariri Crater
Waingongongongo Crater
Hochstetter Crater
Rotomahana East Crater
Rotomahana West Crater
0
1 km

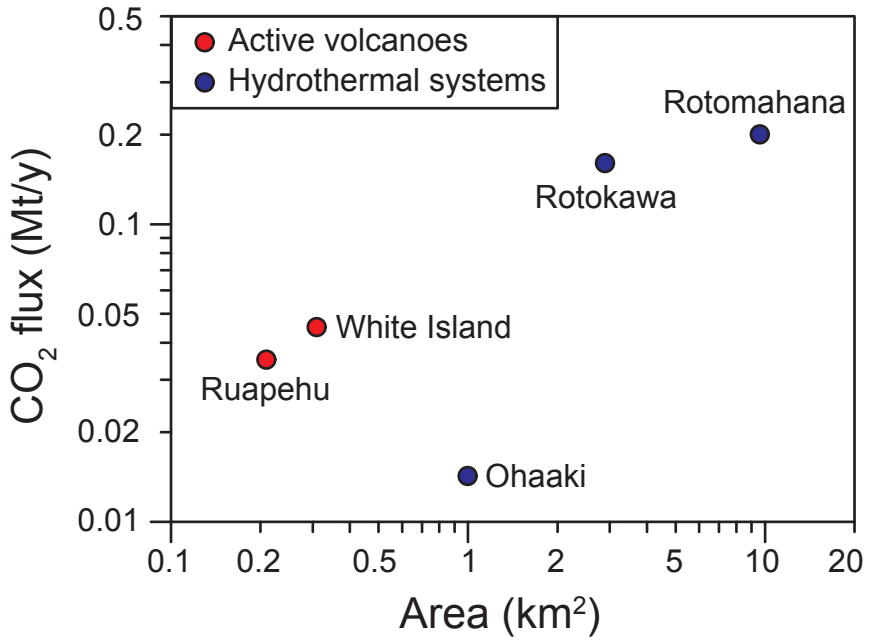
Active volcanoes
Hydrothermal systems
Rotomahana
Rotokawa
White Island
Ruapehu
Ohaaki
0.5
0.2
0.1
0.05
0.02
0.01
0.1
0.2
0.5
1
2
5
10
20
CO2 flux (Mt/y)
Area (km2)

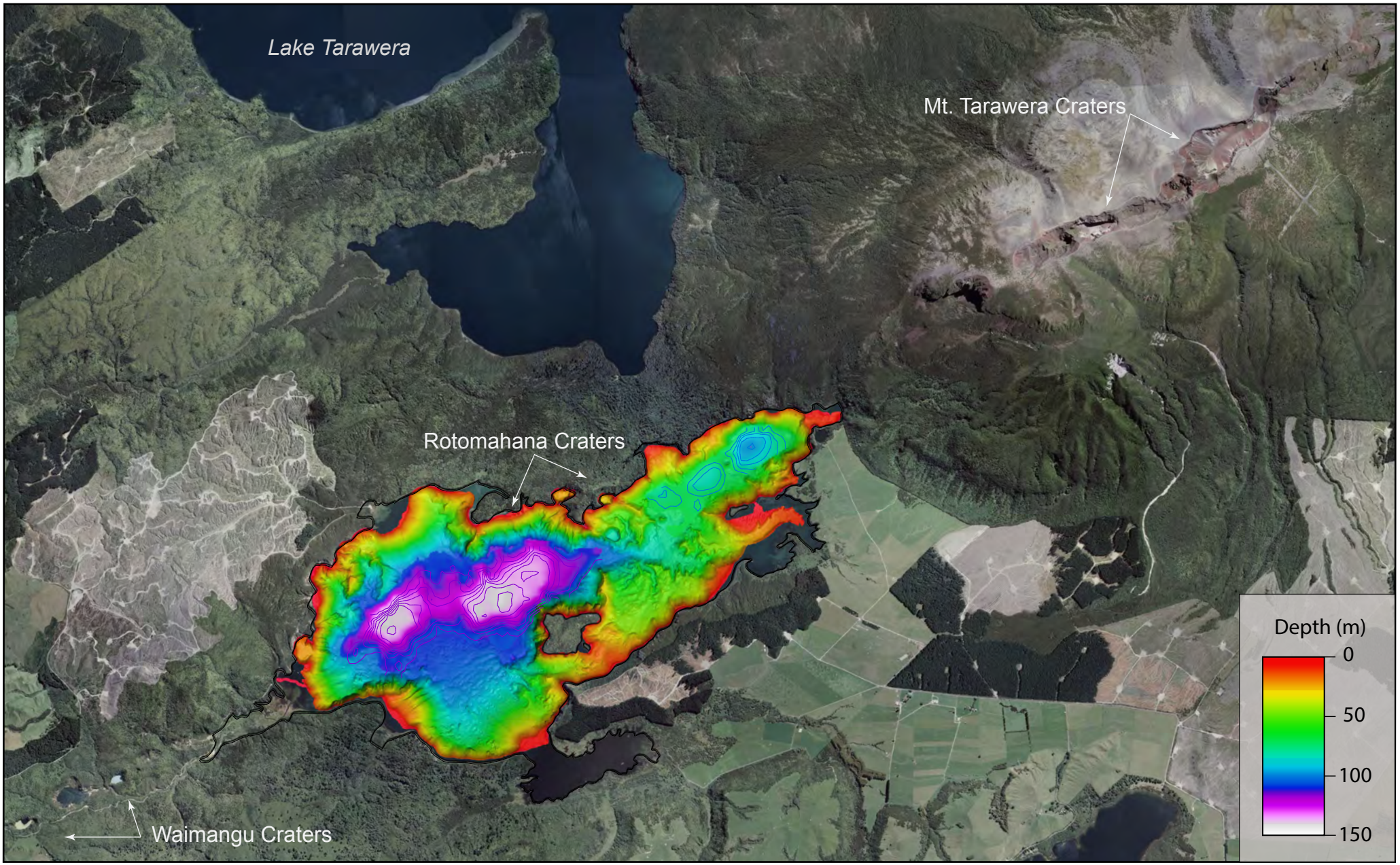
Lake Tarawera
Mt. Tarawera Craters
Rotomahana Craters
Waimangu Craters
Depth (m)
0
50
100
150

Table 1: Rotomahana explosion crater statistics from high-resolution bathymetry

Crater[1] Type	Crater[2] Diameter (m)	Crater[3] Depth (m)	Diameter/ Depth[4]	Comments
Small	37	6.8	5.4	
Small	50	9.6	5.2	
Small	61	12.4	4.9	
Small	62	7.6	8.2	
Small	70	16.4	4.3	
Small	82	9.6	8.5	
Small	85	20.4	4.2	
Medium	146	27.8	5.3	
Medium	158	52.1	3.0	
Medium	162	34.1	4.8	Smith Crater
Large	332	71.4	4.7	Otukapuarangi Bay Crater[5]
Large	335	84.4	4.0	Top of crater is subaerial
Large	337	79.7	4.2	Star Hill Crater[5]
Large	355	1.5	236.7	
Large	452	67.4	6.7	Donne Crater[5]

1, Crater type is based on three obvious distributions of crater diameter; small (37-85 m), medium (146-162 m) and large (332-452 m)
2, Maximum diameter as not all craters circular
3, Depth from rim of crater to floor of crater (i.e., to the surface of any sediment infill); craters with a subaerial component are measured for both their maximum diameter and crater depth from subaerial rim
4, Ratio of crater diameter to crater depth is influenced by degree of sediment infill Criteria for determining a crater include: at least 180° of rim present; mostly circular in shape; margin of crater is defined
5, Top of crater is subaerial
Measurements taken from high-resolution bathymetry (see Fig. 4A) using tools within Feldermaus®. See Figure 4B for location of craters.

Table 1: Lake Rotomahana terraces depths related to 2012 multibeam survey

Terrace	Depth (m) *Profile a-b*		*Profile c-d*	*Profile e-f*	*Profile g-h*	*Profile i-j*	*Profile k-l*	Average depth (m)	Range in depth (m)	Average elevation AMSL[2] (m)	Comments[3]
M	4.4	4.4		4.2	4.1			4.3	0.3	335.6	Lake levels in years 1925 & 1926
L			5.4		5.0			5.2	0.4	334.7	Lake levels in years 1924, 1932 & 1935
K	6.1		6.0	5.9		6.1		6.0	0.2	333.9	
J	7.0		7.1	7.1				7.1	0.1	332.8	
I		8.0			7.9			8.0	0.1	331.9	
H	9.0			9.1	9.5	9.2		9.2	0.5	330.7	Height of Greater Lake Tarawera
G		10.0	10.0	10				10.0	0	329.9	
F	12.8		12.6	12.7	12.3			12.6	0.5	327.3	
E		13.3	13.7	13.4				13.5	0.4	326.4	
D	14.4		14.2	14.0	14.5	14.0		14.2	0.5	325.7	
C		15.8			16.3			16.1	0.5	323.8	
B		16.8				16.6		16.7	0.2	323.2	
A	17.5	17.7	17.6	17.4				17.6	0.3	322.3	
A1						18.7		18.7	0	321.2	A1 is seen only in profile k-l

1, See Fig. 4B for location of terraces profiles with select profiles plotted in Fig. 8
2, Average depth falls within +/- 0.5 m of the given AMSL (above mean sea level) value
3, Historical lake level data, see http://monitoring.boprc.govt.nz/MonitoredSites/cgi-bin/hydwebserver.cgi/sites/details?site=209&treecatchment=26
292 m asl = Pre-1886 eruption lake level at Rotomahana (Keam, this issue)
330 m asl = Greater Lake Tarawera lake level (B.P. 5500)
315 m asl = Greater Lake Tarawera lake level (B.P. 700)
339.885 m asl = Lake level during 2012 multibeam survey